FY 2012 Oklahoma Water Resources Research Institute Grant
Final Technical Report

Title:
Identifying Nutrient Pathways to Streams: Sediment and Phosphorus Loads from Streambank Erosion and Failure in the Illinois River Watershed

Start Date:
March 1, 2012

End Date:
August 31, 2013

Congressional Districts:
03 – Stillwater, Oklahoma State University and Project Sites

Focus Category:
GEOMORPHOLOGICAL PROCESSES, HYDROLOGY, NONPOINT POLLUTION, NUTRIENTS, SEDIMENTS

Descriptors:
Streambank Erosion, Sediment, Phosphorus, Riparian Protection

Principal Investigators:
Garey A. Fox, Ph.D., P.E., Professor and Buchanan Chair, Department of Biosystems and Agricultural Engineering, Oklahoma State University; Chad Penn, Associate Professor, Plant and Soil Sciences, Oklahoma State University; Dan Storm, Professor, Biosystems and Agricultural Engineering, Oklahoma State University

Publications:
Fox, G.A., R.B. Miller, E. Daly, D.E. Storm, and C. Penn. 2013. Streambank and phosphorus loading from protected and unprotected streambanks in eastern Oklahoma. ASABE Annual International Meeting, Conference Proceedings Paper, Kansas City, MO, July 21-24, 2013.

Miller, R.B., G.A. Fox, C. Penn, S. Wilson, A. Parnell, R.A. Purvis, and K. Criswell. 2014. Estimating sediment and phosphorus loads from streambanks with and without riparian protection. *Agriculture, Ecosystems, and Environment* 189: 70-81, doi: 10.1016/j.agee.2014.03.016.

Table of Contents

List of Figures

List of Tables

Summary Table of Student Support

Student Status	Number	Disciplines
Undergraduate	2	Biosystems and Agricultural Engineering
M.S.		
Ph.D.	1	Biosystems and Agricultural Engineering
Post Doc	1	Biosystems and Agricultural Engineering
Total	4	Biosystems and Agricultural Engineering

Abstract

Nutrients and excessive sediment are two main nonpoint source pollutants in the United States. In some watersheds, the majority of the total sediment load to streams and rivers is from streambank erosion. The presence of riparian vegetation can significantly decrease streambank erosion in some locations. Streambank erosion and failure may be one pathway for phosphorus (P) loading to streams, but insufficient data exists on actual loading from this source and the potential protective effect of riparian vegetation in most watersheds. The objective of this research was to characterize the distribution of soil P concentrations in streambanks both with and without implemented riparian protection in the Barren Fork Creek watershed in eastern Oklahoma and to estimate P loading due to bank erosion. Barren Fork Creek is a state-designated Scenic River in Oklahoma where soil P levels are potentially high due to historic poultry litter application. Streambank soil samples were collected at three transects and at four vertical locations at six different reaches. Streambank core samples were collected up to 50 cm into the bank at each location. Also, lateral bank erosion over a seven year period (2003-2010) was estimated using aerial photography. Soil samples were analyzed for pH, electrical conductivity (EC), water-soluble phosphorus (WSP), degree of P saturation (DPS), and total phosphorus (TP). A video reconnaissance of the Barren Fork Creek throughout the entire watershed in Oklahoma was performed to estimate the average percent reach failing. Contour plots of streambank P concentrations illustrated considerable differences among reaches relative to adjacent land use. Average streambank migration rates were approximately 8 m for the three sites with riparian protection compared to 45 m for the three sites without riparian protection over the seven year period. When considering the combination of P concentrations and the extent of erosion as documented by the video reconnaissance (approximately 37.5% failing and unprotected banks), streambanks represent a considerable source of P entering Barren Fork Creek and eventually impacting water supply reservoirs. Total WSP from streambanks on the Barren Fork Creek from unprotected and failing banks was approximately 1540 kg/yr, which represented approximately 10% to 15% of the dissolved P load in the Barren Fork Creek between the Dutch Mills and Eldon gauge stations. Estimated TP load from streambanks was approximately 79,900 kg/yr, which exceeded the TP load estimated in the Barren Fork Creek between the two gauge stations. Unlike WSP the TP is largely sediment-bound and thus subject to sediment transport dynamics such as deposition on point bars and in floodplains. Streambank erosion and bank retreat events were episodic; therefore, there is a need to use bank stability models that consider the physical processes of fluvial erosion and geotechnical stability to model streambank erosion and bank retreat over extended time scales.

Problem Statement and Research Objectives

Nutrients and excess sediment are two of the primary pollutants of surface waters in the United States. Main sources of nutrients include fertilizer, legacy P from discharges in the upper portion of the watershed, and wastewater treatment plant discharge. However, there is currently insufficient data about many of the watersheds to determine the loading of sediment and nutrients from streambanks. Billions of dollars have been spent on streambank stabilization to help slow bank retreat and reduce sediment loading (Lavendel, 2002; Bernhardt et al., 2005). Riparian protection can drastically reduce streambank erosion in locations, but estimates of actual decreases in sediment and P are limited. Understanding the effects of riparian protection on sediment and P loading to streams due to streambank erosion can justify the use and demonstrate the effectiveness of such management practices.

Barren Fork Creek is a fourth order stream, originating in northwestern Arkansas which flows west through the Boston Mountains and Ozark Highlands ecoregions, and reaches its confluence with the Illinois River at Lake Tenkiller near Tahlequah, OK (Figure 1). The Barren Fork Creek watershed is within the Illinois River watershed, which has many areas listed on the 303(d) list for nutrient related impairments. Barren Fork Creek has a natural meander and high degree of sinuosity, but changes in land use over the past 150 yrs may have resulted in accelerated rates of streambank erosion and lateral channel migration. This watershed, which is typical of those in the Ozark ecoregion in eastern Oklahoma, is characterized by cherty soils and gravel bed streams. Streambanks within the watershed commonly are composed of two distinct layers with contrasting textures and properties (Figure 2, Midgley et al., 2012). The top layer is typically a cohesive silt loam soil which can range in thickness from several centimeters to more than a meter. Underlying the topsoil, separated by a very sharp change in texture, is typically a non-cohesive “imbricated” gravel layer, similar in size to the streambed gravel, which also ranges in thickness from tens of centimeters to a meter or more. Also typically present is a gravel “toe” consisting of loose larger gravel particle sizes that have been detached from the imbricated gravel but not yet transported away. Previous research experience within the watershed has shown that the gravel extends downward to the bedrock surface which can be 10 m or more below the ground surface.

Streambanks composed of layers with contrasting textures have been labeled “composite banks” in the literature (Thorne and Tovey, 1981), and exhibit distinct erosional characteristics that can lead to episodes of rapid stream migration. Erosion typically occurs in a sequence beginning when fluvial entrainment of the underlying, unconsolidated gravel produces an undercut bank, which eventually fails when the weight of the unsupported block exceeds the cohesive strength of the soil. It is known that riparian vegetation can affect bank stability, and it is commonly assumed that the strength of plant roots anchored in the banks add some amount of strength to the soil which increases its resistance to mass failure, a force component termed “root cohesion” (c_r). Trees, shrubs and grasses all have roots and thus all presumably contribute to c_r, but trees have a much larger range of root sizes and tensile strengths, all of which persist throughout the seasonal progression each year, and also the

presence and absence of trees provides a large contrast that can be easily determined through aerial imagery. Sites selected for this study include those with and without long-term riparian trees. One supporting goal for the project will be to use the results to help measure the success of recently implemented riparian protection practices in these watersheds.

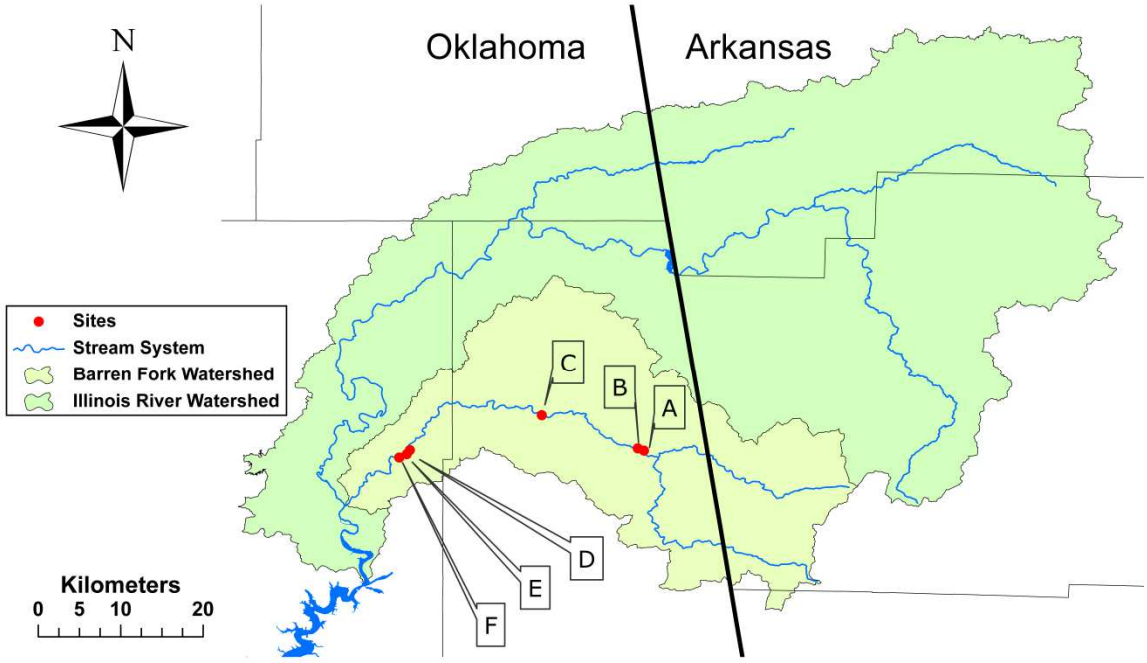

Figure 1. Barren Fork Creek watershed in Oklahoma and Arkansas, and study site locations.

Poultry litter, a by-product of egg and poultry production, has historically been applied as fertilizer within the Ozark region including the Barren Fork Creek watershed. These fertilizers are high in P and excess P concentrations may build up on the soil surface. Runoff of precipitation over the surface immediately after application can lead to the transport of P into the stream. The P can also be sorbed onto the soil, so erosion of the soil surface can lead to a pulse of sediment and sediment-bound P entering the streams (Mittelstet et al., 2011). These processes result in an excess of nutrients within the water and can lead to eutrophication which, in turn, decrease the quality and productivity of the receiving lake and/or water supply reservoir. Streams and water bodies in the eastern Oklahoma Ozarks are very sensitive to nutrient pollution, so determining loading into the waterways is important, but in this effort, bank erosion as a P-load source has often been ignored.

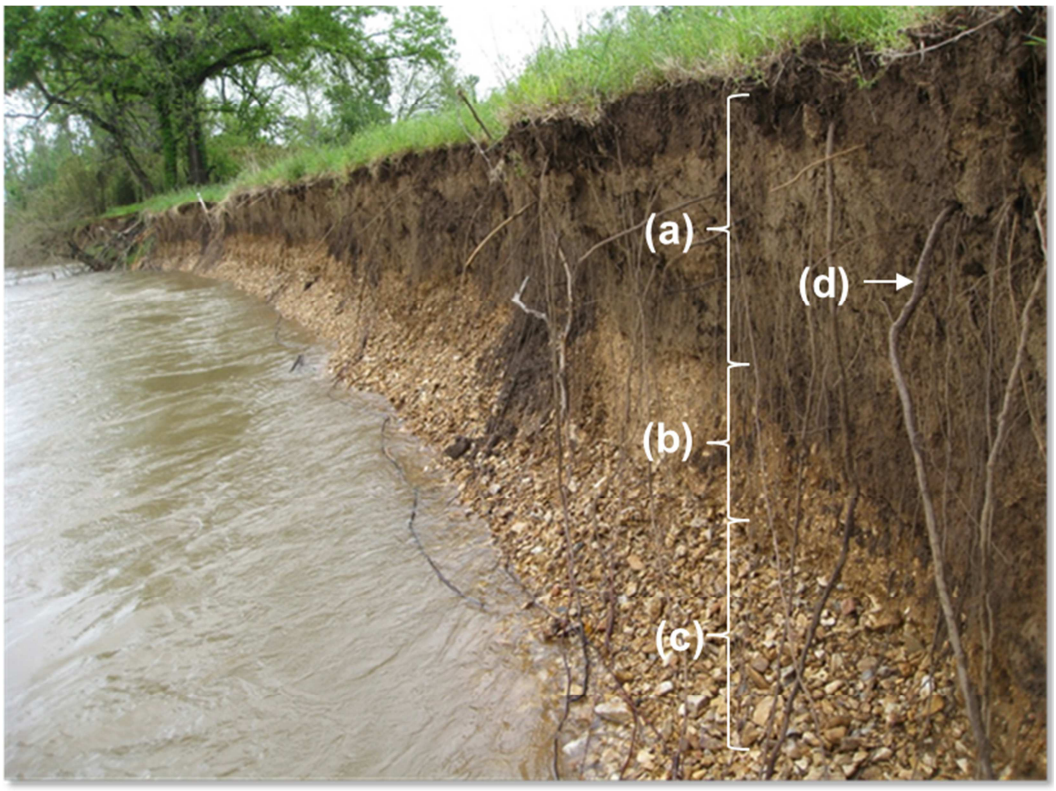

Figure 2. A Barren Fork Creek composite bank showing typical layers: (a) silt-loam topsoil, (b) "imbricated" (packed) gravel, and (c) loose gravel toe. Recent stream migration has eroded into (d) root zone of riparian tree near bank edge (not shown) (Midgley et al., 2012). Note that roots occupy only the cohesive soil layer, and do not extend into gravel layer. The steep bank profile is typical, and indicates that mass failure is the dominant mechanism of streambank erosion, which in this case is controlled by both the rate of fluvial undercutting of the gravel layers, and the strength of cohesive soil and roots.

A streambank site on the Barren Fork Creek (included in this study) has hosted a number of research projects beginning in 2008 and continuing to the current day. Soon after research began it became obvious that episodic events of dramatic bank retreat were occurring, and detailed surveys of bank location showed 7.8 to 20.9 m of bank retreat during the summer of 2009 over a 100 m reach (Midgley et al., 2012; Figure 3). The existence of episodes of dramatic bank retreat among the study sites emphasizes the need to determine the importance of bank erosion on P loading to Barren Fork Creek and to its receiving water, Lake Tenkiller. Bank erosion has been recognized as a source of P to receiving waters in other studies, with estimates ranging from 7-10% of annual TP in Minnesota (Sekely et al., 2002) to 14-24% of TP in Denmark (Laubel et al., 2003). Zaimes et al. (2008) found that P concentrations within streambank soils in Iowa

was fairly constant, but that streambank erosion, and hence sediment and P loading, varied with riparian land use. Kronvang et al. (2012) examined both erosion and deposition within plots of erosion pins, and was able to estimate net P movement and determine that bank erosion was a significant source of P that accounted for 21-62% of annual loads for a Danish stream with cohesive banks, and that bank erosion was significantly lower along reaches with trees and shrubs compared to reaches dominated by grasses.

The objectives of this research were to assess the importance of bank erosion as a source of P loading to the Barren Fork Creek, and to quantify the bank-stabilizing effects of riparian forests. To accomplish this, the study utilized six selected streambanks with varying characteristics and spatially distributed throughout the Barren Fork Creek watershed within Oklahoma to address three major goals: (1) quantify the amount of streambank erosion and failure, (2) quantify the amount of WSP and TP in streambanks and the load of WSP and TP from streambanks in the Barren Fork Creek watershed, and (3) estimate the benefit of riparian management practices in the Barren Fork Creek watershed.

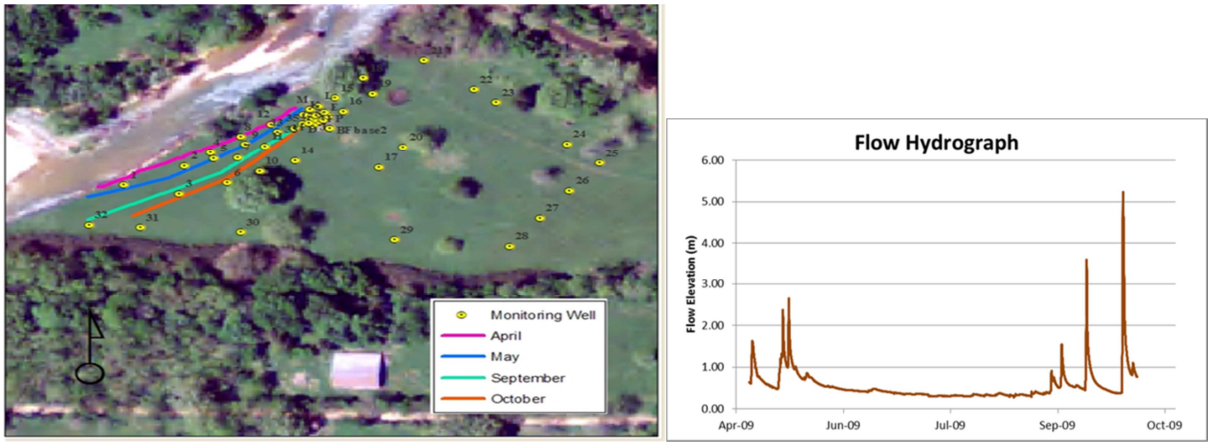

Figure 3. Bank retreat during 2009 at a site on Barren Fork Creek, shown on an aerial image from 2008 (Midgley et al., 2012). Episodes of bank retreat range from 7.8 to 20.9 m along a 100 m stream reach, and coincide with major flow events during the year. Yellow symbols indicate location of monitoring wells installed in floodplain, many of which were lost into the stream over the course of the year.

Methods

Sites

Six sites were selected at locations along Barren Fork Creek, which were designated by letters sequentially A-F starting upstream (Figure 1). Landowners allowed access to the sites (with the exception of site D, where only initial soil P and cross-section surveying was allowed). Three sites (B, C, and D) were known to have significant riparian tree coverage along their banks during the all or part of study period (2003-2010), and will

be referred to as “Protected” sites. The remaining sites (A, E, and F) had only pasture grasses during the study period, and will be referred to as “Unprotected” sites. Streambanks generally are either eroding (active), typified by steep banks that are close to the channel thalweg, or accreting (passive), typified by shallow gradients that are relatively distant from the channel thalweg. For this study only active banks were selected. A representative length of bank (reach) was identified at each site that had generally common characteristics including bank height and stratigraphy, and riparian cover.

At each site a reresentative cross section was selected and a detailed bank stratigraphy prepared. A survey of the bank stratigraphy and stream channel was performed using a laser level or total station, and detailed notes kept of the thickness and texture of each bank bank layer, and the stream thalweg (deepest point in channel), as shown in Table 1. Additionally, a particle count was performed for each gravel-dominated layer in the cross-section, including (if present) the imbricated (packed) gravel, loose gravel toe and stream bed gravel. The stream slope along the reach was also measured by surveying the elevation drop along the thalweg from a riffle crest above the reach to one below the reach.

Site A

Site A (Latitude 35.91027, Longitude -94.58778) is historically unprotected and has been used for both pasture and row crops. The site experienced significant bank retreat during the period of study (Table 1, Figure 4).

Table 1. Surveyed characteristics of study sites.

Site	Watershed Area (km^2)	Reach Length (m)	Reach-Averaged Total Retreat (m)	Total bank height (m)	Cohesive soil thickness (m)
A	363	190	33.7	2.80	1.58
B	364	233	8.0	2.72	0.93
C	544	138	7.3	4.57	2.16
D	829	182	8.0	2.25	0.58
E	830	185	68.3	2.88	0.77
F	845	190	33.7	3.15	1.31

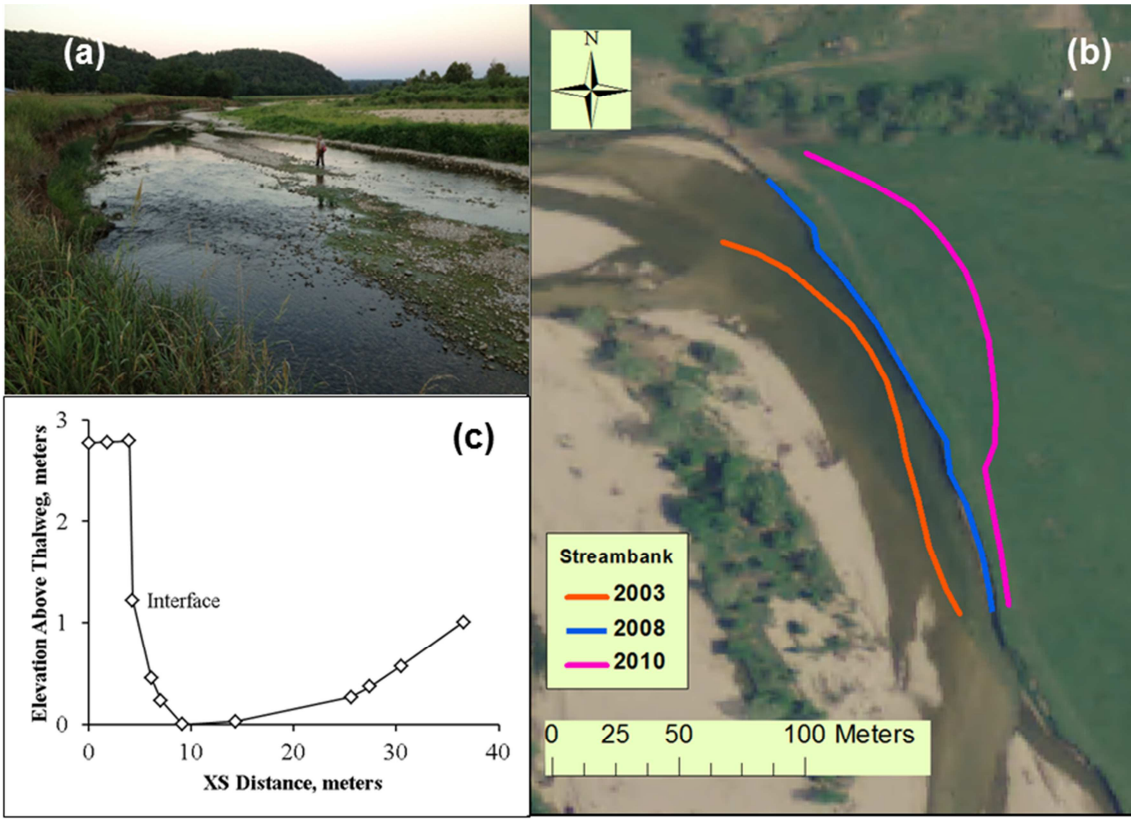

Figure 4. Site A images: (a) view of bank looking upstream, (b) bank positions from NAIP imagery (2008 shown), indicating dramatic bank retreat, and (c) surveyed bank profile at cross-section showing cohesive soil/gravel interface.

Site B

Site B (Latitude 35.91277, Longitude -94.59451) is historically protected and was not utilized for agricultural activities during the study period. Slight, but measureable bank retreat was noted during the study period (Table 1, Figure 5).

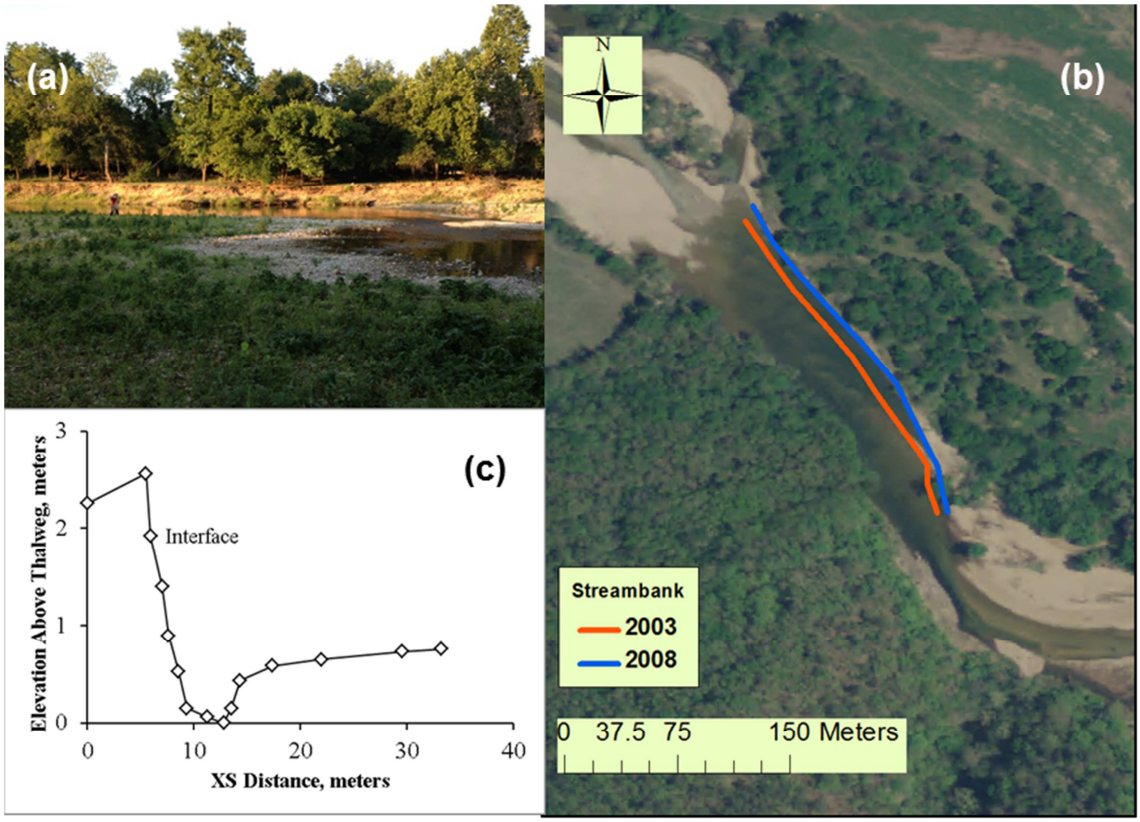

Figure 5. Site B images: (a) view of bank looking downstream and showing riparian forest cover typical of reach, (b) bank positions from NAIP aerial imagery showing retreat during 2003-2008 interval only (no retreat detected 2008-2010), and (c) surveyed bank profile showing cohesive soil/gravel interface.

Site C

Site C (Latitude 35.94878, Longitude -94.6993) is a pasture that was historically protected by a strip of riparian trees. During the study period a portion of the riparian forest was eroded away. Erosion was detected in NAIP aerial imagery in the interval 2003-2008, but not 2008-2010 (Table 1, Figure 6).

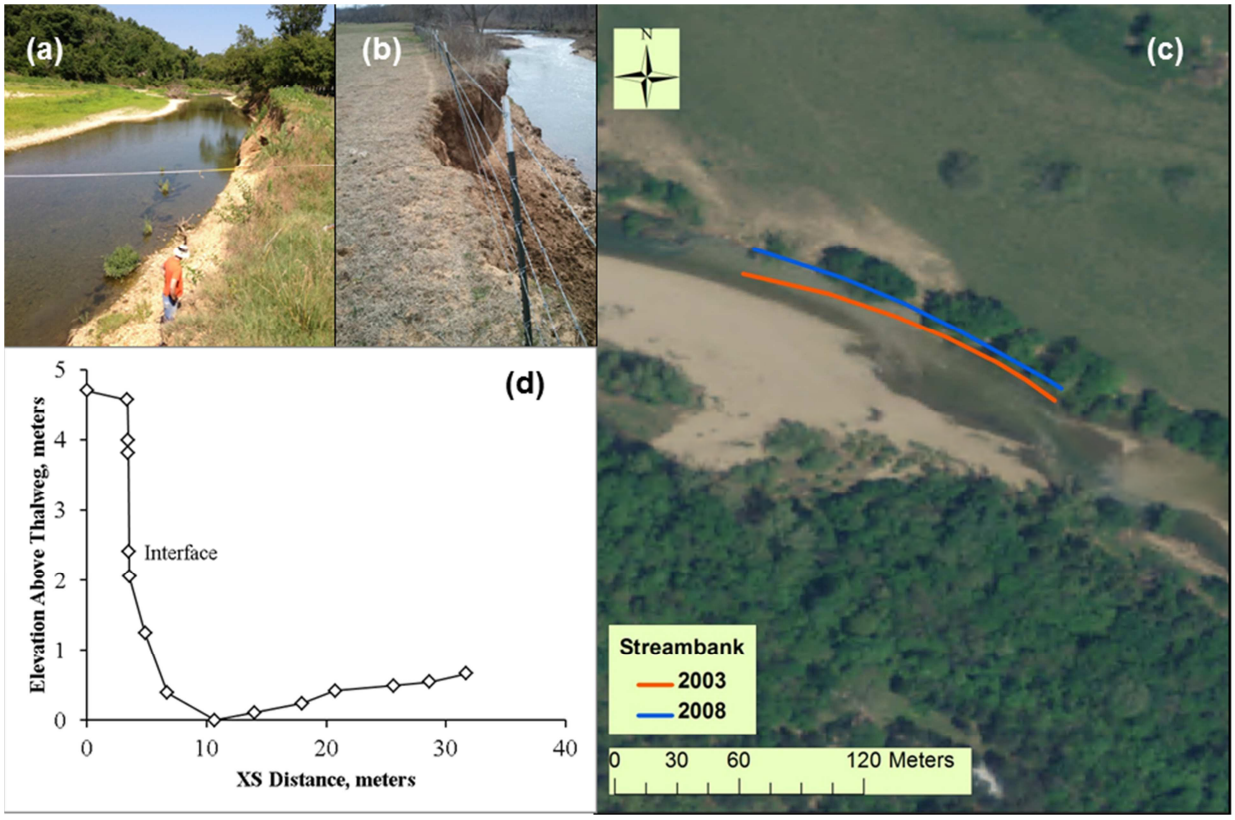

Figure 6. Site C images: (a) view of eroding Bank looking downstream, (b) detail of recent (since 2010) undercutting of fence line, (c) bank locations from NAIP imagery (no retreat observed from 2008-2010), and (d) surveyed bank profile showing cohesive soil/gravel interface.

Site D

Site D (Latitude 35.91085, Longitude -94.8431) is a historically protected site with an established riparian forest. Erosion is evident on NAIP aerial imagery in the interval 2003-2008, but not 2008-2010 (Table 1, Figure 7).

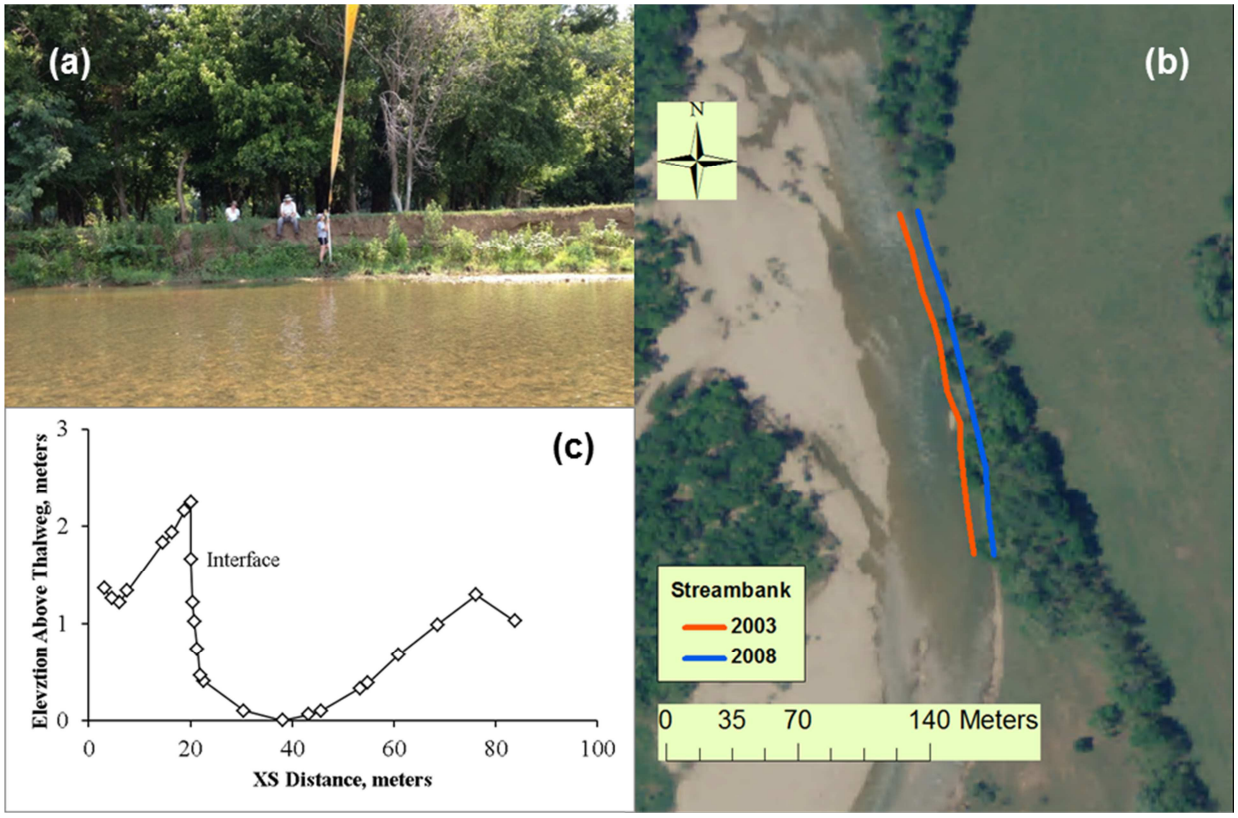

Figure 7. Site D images: (a) view of bank showing mature riparian forest, (b) bank locations from NAIP aerial imagery (no retreat observed from 2008-2010), and (c) bank profile showing cohesive soil/gravel interface.

Site E

Site E (Latitude 35.90633, Longitude -94.8465) is a historically unprotected site dominated by pasture. The site has been used for grazing cattle and horses. Dramatic rates of erosion were evident in the intervals 2003-2008 and 2008-2010 (Table 1, Figure 8).

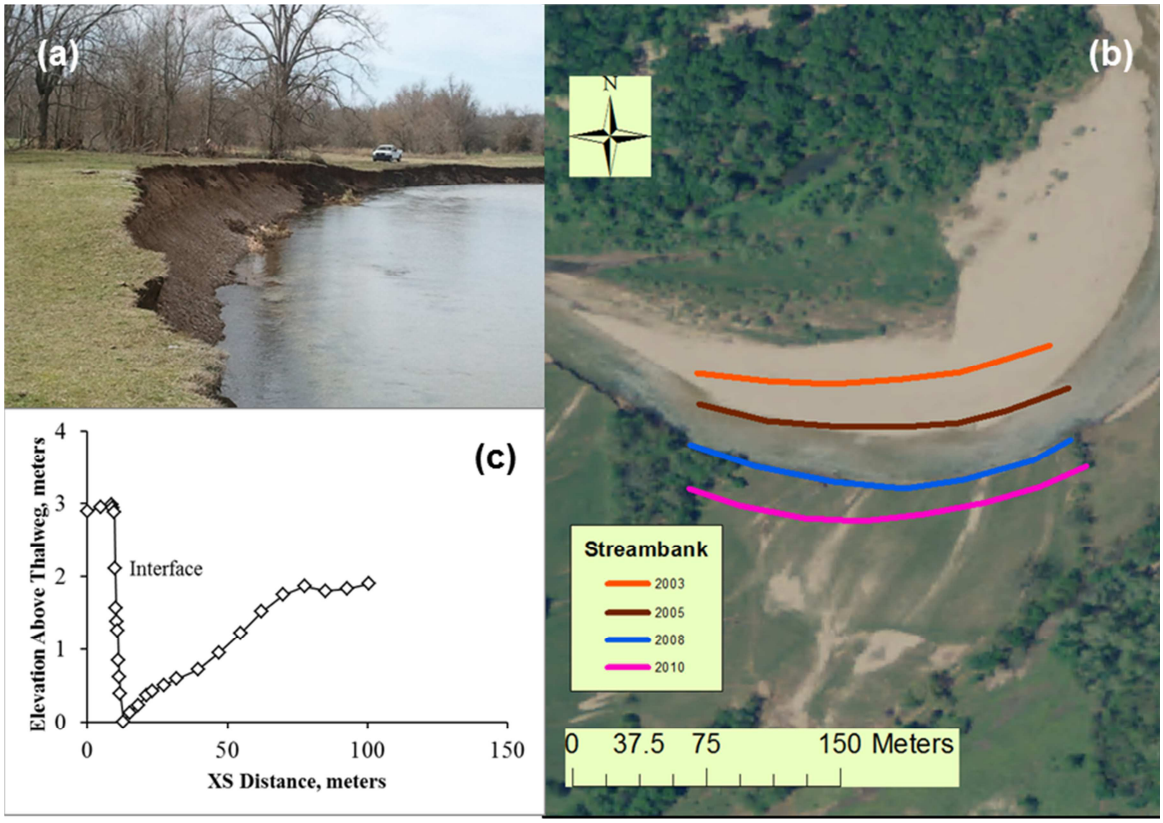

Figure 8. Site E images: (a) view of bank looking upstream and showing recent failed blocks at base of bank, (b) bank positions from NAIP (2008 shown) imagery showing very dramatic bank retreat in the interval 2003-2008, and lesser but significant retreat 2008-2010, and (c) bank profile showing cohesive soil/gravel interface.

Site F

Site F (Latitude 35.90276, Longitude -94.8548) is a historically unprotected site dominated by pasture. The site has been used primarily as a hayfield. Dramatic rates of erosion were evident in the intervals 2003-2008 and 2008-2010 (Table 1, Figure 9).

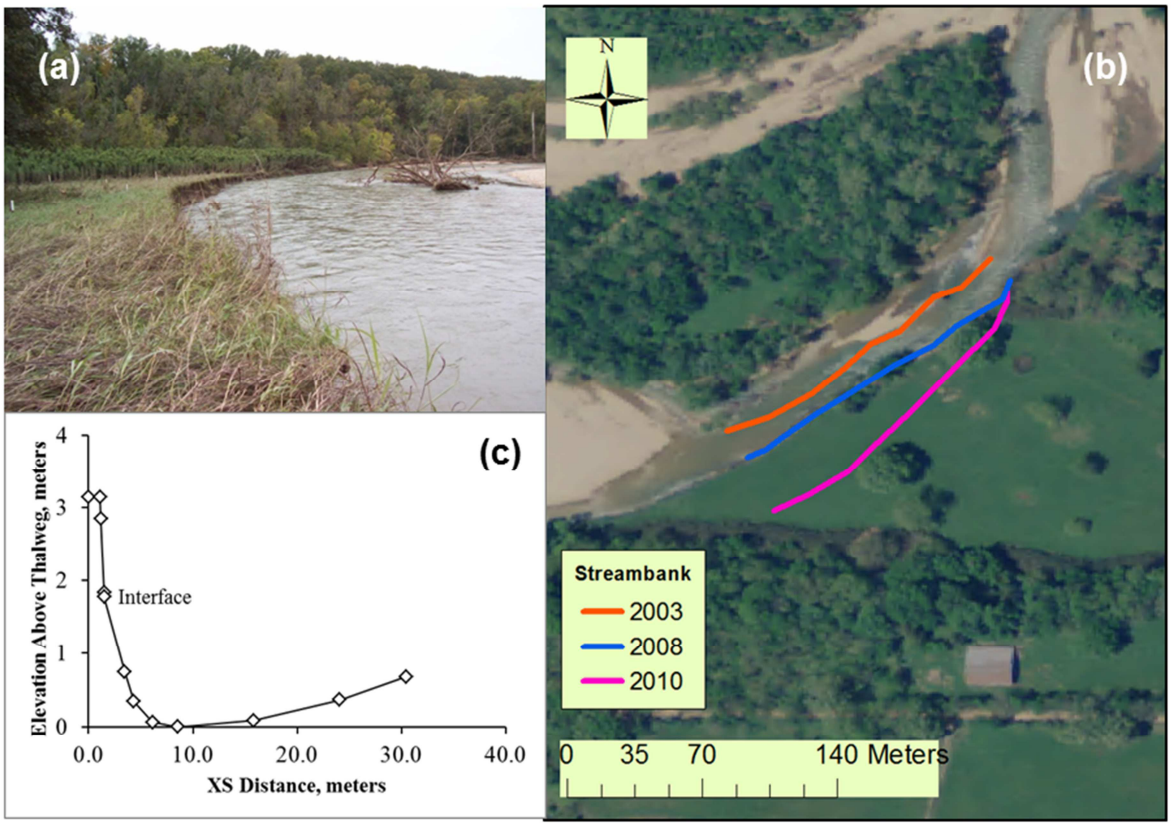

Figure 9. Site F images: (a) view downstream showing steep eroding bank, (b) bank positions from NAIP aerial imagery (2008 shown) indicating significant erosion in 2003-2008 and 2008-2010 intervals, and (c) bank profile showing position of cohesive soil/gravel interface.

Streambank Testing

The resistance of the streambanks' to geotechnical failure and fluvial erosion were quantified. Soil strength (*S*, kPa) or the resisting force which is responsible for bank stability is usually defined using the modified Mohr-Coulomb's equation (Simon et al., 2000):

$$s_r = c' + \sigma \tan(\phi') + \psi \tan(\phi^b) \quad (1)$$

where *c'* is effective cohesion (kPa), σ is the normal stress (kPa), ϕ' is the internal angle of friction (°), ψ is the matric suction (kPa), and ϕ^b is an angle that describes the relationship between shear strength and matric suction (degrees). Fredlund and Rahardjo (1993) assume ϕ^b to be between 10 and 20 degrees and that ϕ^b approaches ϕ' at saturation. The soil strength parameters *c'* and ϕ' of the cohesive soils were measured *in situ* using the borehole shear test (BST, Handy Geotechnical Instruments, Inc., Madrid, IA). The BST includes a shear head, which is inserted into a prepared

borehole and expanded with a CO_2 pressure cylinder. This expansion causes a block of soil surrounding the shear head to consolidate. After allowing the soil water to re-equilibrate within the soil block, the test is performed by increasing the shear force until the consolidated soil block shears from the native soil. By sequentially increasing the normal stress and recording the shear stress a typically linear dataset is created in which the apparent cohesion corresponds to the y-intercept (kPa) and the ϕ' corresponds to the slope of the fitted line. The ψ was measured at a later time with a tensiometer from a sample acquired in the field, and the value applied to estimate *c'*. The unconsolidated gravels within the streambanks do not have cohesive strength and are only represented by a frictional resistance through ϕ', which was calculated from the median particle size (d_{50}) observed at each site.

Typically the fluvial erosion rate of cohesive soils is quantified using an excess shear stress equation, dependent on the critical shear stress (τ_c) and the erodibility coefficient (k_d). A submerged jet test apparatus is one of the best methods for measuring these parameters *in situ*, and has been used extensively for estimating the excess shear stress parameters for use in modeling streambank resistance to fluvial erosion (Hanson, 1990; Simon et al., 2010; Al Madhhachi et al., 2013). The "mini" jet test device was positioned on the face of the streambank in cohesive soil layers (i.e., silt loam above the gravel). The τ_c for unconsolidated gravel layers was estimated based on the average gravel particle size using the Shield-Yalin diagram. Estimates of k_d for the unconsolidated gravel based on the estimated Shield-Yalin τ_c were calculated from previous k_d-τ_c correlations (e.g. Simon et al., 2010), and from previous bank modeling on similar sites (Midgley et al., 2012).

Root Biomass

The contribution of tree roots to the cohesion of the cohesive streambanks was not directly measured in this study. Instead the below-ground root biomass was estimated at each forested site in the following manner. First, the species and diameter at breast height (DBH) was determined within a known area at each site; generally this included all trees within 5 m of the bank edge and within a 100 m distance along the reach. Next, the above-ground biomass (AGB) of each tree was estimated using the species-specific diameter based allometric equation (Jenkins et al., 2004), if available, or with a similar allometric equation intended for "general hardwoods". The AGB was used in a diameter based ratio to estimate below-ground coarse root biomass (BGB) with the following equation (Jenkins et al., 2004):

$$\frac{AGB}{BGB} = Exp\left(-1.5619 + \frac{0.6614}{DBH}\right) \quad (2)$$

Finally, a root biomass per soil volume estimate was calculated by dividing the BGB by the biomass survey area times the cohesive soil depth from the channel cross section.

Aerial Imagery Analysis

Images from the National Agricultural Imagery Program (NAIP) from 2003, 2008 and 2010, all with 1 m horizontal resolution, were obtained for analysis. The images were

georeferenced in ArcMap 10 (ESRI, Redlands, CA) and then used for determining bank erosion over time (Figure 10) following Heeren et al. (2012). A bounding rectangle, corresponding to the field-determined reach length, was created for each site. Within the rectangle, the bank edge for each NAIP image was digitized. Erosion was determined to have occurred when the digitized bank for the next NAIP appeared to be farther from the stream centerline than the previous bank. When erosion was determined to have occurred, a polygon was created using the two digitized bank locations, and the area calculated in square meters. The total bank retreat was the area of the polygon (TR, m^2); reach-averaged lateral retreat (SR, m) was the area divided by the reach length. Total sediment loading (*SL*, kg or kg/yr) into the stream from each site was then determined using the estimated reach length (*RL*, m), the average lateral streambank retreat (*SR*, m), soil bulk density (ρ_b), and depth of the topsoil from cross-section surveys (D_{ts}, m):

$$SL = RL \times SR \times D_{ts} \times \rho_b \quad (3)$$

Additionally, the aerial imagery was used to estimate the radius of curvature (*ROC*) at each stream reach by drawing a circle with a perimeter overlying the bank edge and then adjusting the circle diameter until the match between the bank edge and perimeter were as close as possible. The radius of the circle was then calculated in meters.

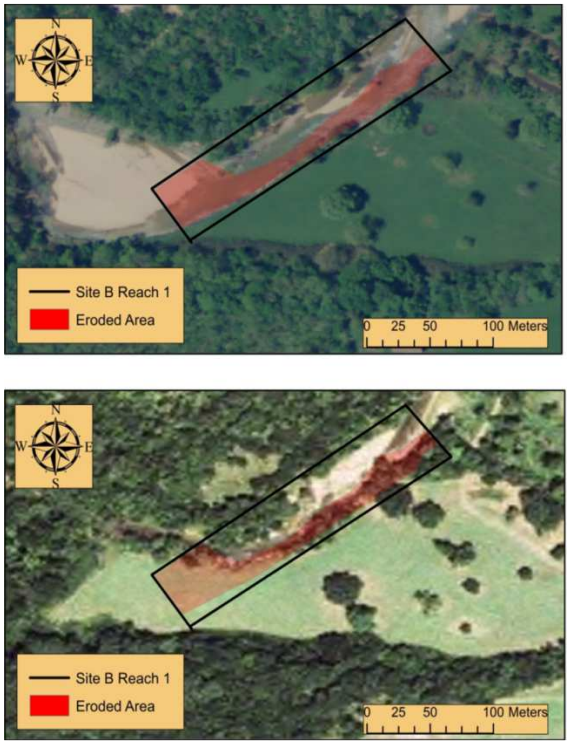

Figure 10. NAIP aerial images from 2003 (bottom) and 2008 (top) of a stream and the polygon (in red) showing the area of bank eroded during that time period.

Aerial Survey
A video aerial reconnaissance of the Barren Fork Creek streambanks was performed as part of a different project funded by the Oklahoma Water Resources Board and Oklahoma Conservation Commission. This survey was performed by flying a helicopter to obtained GPS-linked video of both streambanks along the length of Barren Fork Creek within Oklahoma. The video was then analyzed to determine the length of banks that exhibited unstable characteristics, such as steep slopes, or the presence of failed blocks at the bank toe. The 55 km of stream (110 km total streambank length) was then divided into 2-km increments, which were classified by the average percent of the increment that was unstable and actively failing.

Soil P Collection
At each study site soil samples were collected using a 50 by 2.54 cm soil corer driven horizontally into the bank face. The following procedure was used to measure the distribution of P vertically within the cohesive soil layer and horizontally away from the bank face.

- Within each site, three locations (transects) were identified, with similar soils and bank layer thickness.
- At each transect soil cores were obtained with the following vertical distribution:
    - near the bank surface (5 and 15 cm, vertically from surface)
    - middle of the silt loam topsoil depth (~60 cm, vertically from surface)
    - just above the interface between the topsoil and gravel layers (~90 to 120 cm)
- The sampler was driven 50 cm into the streambank face (or to refusal), and then divided into three sections (subsamples) as measured from the bank face
    - 0 to 5 cm
    - 5 to 20 cm
    - 20 to 50 cm.
- For the topmost samples, it was possible to extend the horizontal sampling depth to approximately 1 m from the bank face by driving the sampler vertically into the soil and dividing the resulting sample to match the horizontal core depths (5 and 15 cm).

Soil samples were acquired in June 2012. Subsamples were labeled in the field and refrigerated until they were delivered to the soil chemistry laboratory. Subsamples were analyzed individually (not composited). Once delivered to the soil chemistry laboratory, subsamples were air-dried and ground to uniform particle size.

Analysis of Soil Chemistry
Subsamples from the cores were characterized for soil test phosphorus (STP), WSP, DPS, TP, and soil properties that impact P saturation (e.g., pH and EC).

Soil pH was measured by weighing out 5 g of soil from the core subsample and adding 15 mL of distilled water (DI water) to a vial to obtain a 1:3 (soil:water) ratio required for the tests. Vials were shaken for 30 seconds, ensuring that all soil was wet. Samples were then equilibrated for 20 minutes and were shaken again. After sitting for another 20 minutes the calibrated pH probe was placed into the sample mixture. Once the probe had stabilized, the reading was taken to the nearest 0.01. The probe was rinsed with DI water between each sample. The same sample preparation procedure was used for EC, using a calibrated EC meter.

The WSP is an estimate of the amount of P that is readily available for plant uptake. A 2 g subsample of soil was weighed and placed with 20 mL of DI water into a centrifuge tube, and all tubes were placed on a shaker platform at the low setting for an hour. After shaking, samples were centrifuged at 2000 rpm for 13 minutes. Each solution was then individually vacuum filtered using 0.45-µm filters. The P concentrations in the filtered solutions were determined using the Murphy Riley colorimetric method (Murphy and Riley, 1962). The procedure used 5 mL of the Murphy Riley reagent in each sample. Test tubes were left to equilibrate for 30 minutes and then analyzed, against standards, using a spectrophotometer. This test is the most appropriate environmental estimator of P concentrations in runoff as compared to other soil test methods (Fuhrman et al., 2005). Dissolved reactive P concentrations in runoff are correlated to a soil's WSP (Pote et al., 1996).

In many soils, including those in the study area, the sorption of P is controlled by the amount of amorphous aluminum (Al) and iron (Fe) oxides present in the soil. Degree of phosphorus saturation (DPS, %) is a common indicator of the potential of a soil to release P to water is calculated as the following:

$$DPS = \frac{P_{ox}}{\alpha(Fe_{ox}+Al_{ox})} \times 100 \quad (4)$$

which is the ratio of P_{ox}, ammonium oxalate extractable P (mol/kg) to the sum of Fe_{ox} and Al_{ox} (ammonium oxalate extractable Fe (mol/kg) and Al (mol/kg), respectively), expressed as a percent (Houben et al., 2011). The α is an empirical constant intended to account for the proportion of Al and Fe oxides that can effectively sorb P, and is commonly assumed to be 0.5.

The STP refers to soils tests designed to estimate the plant-available P in soils. The Mehlich-3 test is the usual test for this purpose in Oklahoma (Mehlich, 1984; Fuhrman et al., 2005). This test does not directly address the release of P to water, but is widely performed on agricultural soils, and thus allows the study results to be easily compared to commonly available data.

The TP was measured using EPA method 3051a (EPA, 2007), in which a soil sample is digested by microwave heating in a solution of HCl and Nitric acids, then the P concentration of the extractant determined using Inductively-coupled Plasma Mass Spectrometry (ICP-MS).

Soil P data were reported in two ways. First, site averages for the various P analyses were determined by calculating the mean of all subsamples from the three transects. This value generalized spatial and concentration variation at the site and was used for comparisons among sites and to calculate loading estimates. Total WSP (kg) and TP (kg) contributed at each stream site was calculated as total mass of eroded topsoil (SL, kg or kg/yr) multiplied by the average WSP and TP for all measurements in the streambank (WSP_{avg}, mg WSP/kg soil, or TP_{avg}, mg TP/kg soil). The length-averaged WSP-load or TP-load for each site was calculated as WSP_{avg} or TP_{avg} divided by the reach length (WSP_{avg} /m or TP_{avg}/m). Average contributions for both unprotected and riparian protected sites were then compared to estimate the benefit of riparian vegetation in preventing WSP or TP loading to the creek. Estimated streambank erosion WSP and TP loads to the Barren Fork Creek were calculated using the length of unstable banks and the estimated WSP_{avg}/m/yr and TP_{avg}/m/yr for unprotected banks from this study.

Secondly, it was possible to portray the two-dimensional spatial distribution of the P in the banks by utilizing the depth below ground surface and the distance into the bank recorded for each sample as spatial coordinates. These data were contoured using SigmaPlot (v 11, Systat Software, Inc., San Jose, CA). Hypotheses, based on the plots, could be made as to the origin of P in the floodplain soil; for instance, relatively high concentrations of P at the bank face may indicate that the stream contributes to floodplain P through sorption of dissolved P from high flood stages.

Load Estimator

The Load Estimator model (LOADEST, Runkel et al., 2004) is a USGS program that estimates annual loads of water-borne constituents, including dissolved P and TP, based on the concentrations of grab samples and the daily hydrograph from USGS gauges. The program creates a linear regression model to predict the log of instantaneous load based on one or more inputs variables including discharge, which takes the general form:

$$\ln(L) = a_0 + \sum_{j=1}^{NV} a_j X_j \quad (5)$$

where L is an estimate of instantaneous load, a_0 and a_j are model coefficients, X_j are the dependent variables, and NV is the number of explanatory variables. The constituent load is the sum of the retransformed predicted instantaneous loads. LOADEST automatically creates several multiple regression models and selects the best model from those from those based on the lowest Akaike Information Criterion statistic. Hydrographs for the period 2003-2010 and P constituent data from the Barren Fork Eldon gauge (Eldon, 07197000, Latitude 35.9211, Longitude 94.8383), and the Barren Fork Dutch Mills gauge (Dutch Mills, 07196900, Latitude 35.8800, Longitude -94.4863) were obtained and modeled with LOADEST. These gauges are situated well for estimating loads within the Oklahoma length of Barren Fork Creek; Eldon is relatively close to the confluence with the Illinois River, and integrates nearly the entire watershed in both Oklahoma and Arkansas, and Dutch Mills is located nearly on the

Oklahoma/Arkansas border, so the Oklahoma Barren Fork will be the difference of loads derived from these sites. The water constituent measured at the gauge that is similar to WSP is “Orthophosphate, filtered, as phosphorus” (constituent 0671), and that similar to TP is “Phosphate, water, unfiltered” (constituent 0650).

The LOADEST estimate is a linear regression-based method, and thus the coefficient of determination (R^2) is an appropriate measure of the linearity of the output relative to the input data; however, linearity itself is not sufficient for gauging the model, since a high R^2 does not imply similarity between observed and predicted values. The quality of hydrologic model predictions is often gauged with the Nash-Sutcliffe Efficiency statistic (NSE, Krause et al., 2005):

$$NSE = 1 - \frac{\sum_{i=1}^{n}(O_i - P_i)^2}{\sum_{i=1}^{n}(O_i - \bar{O})^2} \quad (6)$$

where *O* is the observed concentration and *P* the predicted concentration at time *i*, and *n* the total number of observed concentrations. The NSE ranges from -∞ to 1, with 1 indicating perfect agreement between modeled and observed concentrations, values near 0 imply that the model is no better than using the average of the data. Values less than zero indicate that the residual variance is much greater than the data variance, and the model is a poorer predictor than the average.

Bank Erosion Modeling

Streambank stability models are commonly utilized to investigate the primary mechanisms of bank instability and propose strategies for stabilizing streambanks. One of the most commonly used and most advanced streambank stability models is the Bank Stability and Toe Erosion Model (BSTEM), developed by the National Sedimentation Laboratory in Oxford, Mississippi (Simon et al., 2000). BSTEM has been continually modified and improved by the authors since its creation. The most current public model is BSTEM version 5.4 and consists of two different components: a bank stability module and a toe erosion module, and the capability to model a continuous hydrograph by sequentially applying the various model components, redrawing the bank profile, and then moving to the next step of the hydrograph.

To model bank stability, BSTEM calculates a factor of safety (FoS) using three different limit equilibrium-method models: horizontal layers, vertical slices, and cantilever shear failure. Across horizontal layers, the model accounts for up to five user-input soil layers with unique geotechnical properties. Along vertical slices, the model examines the normal and shear forces active in slices of the failure blocks (portions of the bank above the failure surface). In general, the FoS is calculated as the ratio between the resisting forces and the driving forces along a potential failure plane. The resisting forces can be defined by the modified Mohr-Coulomb equation (equation 1). With unsaturated conditions, soil shear strength is increased by matric suction (Darby and Thorne, 1996; Crosta and di Prisco, 1999; Darby et al., 2007).

Soil weight is the dominating driving force defined by

$$s_d = W \sin(\beta) \tag{7}$$

where s_d is the driving stress (kPa), W is the weight of the wet soil block per unit area of failure plane (kN m^{-2}), and β is the angle of the failure plane in degrees (Simon et al., 2000). Various combinations of failure plane angle and shear emergence elevation (on the bank face) must be considered in order to determine the failure plane with the lowest FoS, which is the plane on which failure is assumed to occur when FoS approaches unity. Recent versions of BSTEM include a subroutine that uses an iterative procedure to automatically determine this information. In summary, the following soil properties influence bank stability and must be estimated or measured: effective internal angle of friction (ϕ'), effective cohesion (c'), unit weight (W), pore-water pressure (μ_w) or matric suction (ψ), and the angle ϕ^b.

The toe erosion component of BSTEM estimates bank undercutting as a result of fluvial erosion (Simon et al., 2000). The model predicts erosion based on an excess shear stress equation originally proposed by Partheniades (1965). Erosion rate, ε (m s^{-1}), is calculated as

$$\varepsilon = k_d (\tau_o - \tau_c)^a \tag{8}$$

where k_d is the erodibility coefficient (m^3 N^{-1} s^{-1}), τ_0 is the average shear stress (kPa), τ_c is the soil's critical shear stress (kPa), and a is an exponent usually assumed to be unity. The k_d and τ_c are lumped parameters that are functions of numerous soil physical properties. For non-cohesive soils, the critical shear stress is typically estimated based on the median particle diameter of the soil (Garcia, 2008). Rinaldi et al. (2008) noted the difficulty in estimating k_d and that no direct methods exist for estimating this parameter. The k_d and τ_c are difficult to approximate for cohesive soils but can be estimated using various methods. One of these methods is a procedure developed by Hanson (1990) using an in situ jet-test device.

The average shear stress (kPa) in BSTEM is calculated using the following equation assuming steady, uniform streamflow (Simon et al., 2000):

$$\tau_o = \gamma_w RS \tag{9}$$

where γ_w is the unit weight of water (9.81 kN m^{-3}), R is the hydraulic radius (m), and S is the channel slope (m m^{-1}). BSTEM divides the bank profile into 23 separate nodes. For each of these nodes, BSTEM calculates τ_0 depending on the segment of flow affecting each node. This method creates a distribution of boundary shear stresses and not just one average shear stress applied over the entire bank. This is still a simplification of the actual shear stress distribution which can be affected by secondary flow and three-dimensional effects in the near-bank zone (Pizzuto, 2008). Papanicolaou et al. (2007) suggested that due to secondary currents the bottom half of the streambank may

experience stress distributions two to three times higher than the shear stress calculated by first order approximations. In BSTEM, the boundary shear stress can be corrected for the effects of curvature using the "no-lag kinematic model" (Crosato, 2007):

$$\tau_o = \frac{\gamma_w n^2 (u+U)^2}{R^{1/3}} \quad (10)$$

where *n* is Manning's roughness coefficient, *u* is the reach-averaged water velocity (m s^{-1}), and *U* is the increase in the near-bank velocity due to superelevation (m s^{-1}).

BSTEM is composed of multiple tabs for inputting geometric, soil, and hydraulic properties and outputting model results. The "Input Geometry" tab contains fields to input the bank profile, soil layer thickness, and channel and flow parameters. Up to five distinct soil layers can be defined with up to 23 points to define the bank profile. Soil properties for each soil layer indicated on the "Input Geometry" tab are input in the "Bank Material" tab. Users can select default soil parameter values for a given soil type or input user defined values. This tab also contains calculations for estimating τ_c based on particle diameter and estimating k_d based on τ_c (Hanson and Simon, 2001).

Model Calibration

BSTEM inputs included the soil strength, erosion resistance, and root cohesion parameters (if applicable), as well as the stream hydrographs for the period 2003-2008. Site-specific rating curves to determine stream depth at thalweg from discharge recorded at Barren Fork Creek USGS gauges were developed with data from in-stream pressure transducers, and adjusted using the proportionality between the gauge and site watershed areas. The field-determined bank characteristics (i.e., erosion and geotechnical resistance parameters of the streambanks) were averaged and those values used as initial estimates for BSTEM. Bank retreat results from the BSTEM model runs were compared with the *SR* as determined by aerial imagery analysis. With fluvial erosion on stream bends being a dominant driving force of retreat, the erosion resistance parameters were used as calibration parameters to match aerial estimated retreat. An alpha factor (α, dimensionless) was used to adjust equation (8) to systematically increase ε and simulate the increased bank erosion resulting from stream curvature:

$$\varepsilon = \alpha k_d \left(\tau_0 - \frac{\tau_c}{\alpha} \right)^a \quad (11)$$

The *α* is directly proportional to k_d and indirectly proportional to τ_c, producing an increased k_d and decreased τ_c for any α greater than one. The *α* was used in situations where initial BSTEM modeled retreat was less than *SR*.

When the BSTEM bank retreat was greater than *SR*, the τ_c of the cohesive soil layer was increased to no larger than the largest field-recorded value, and then the k_d of that layer was decreased until the BSTEM bank retreat was within 0.5 m of *SR*. Additionally the topmost horizontal layer for all of the sites was modeled as an erosion-resistant thatch of grass at the floodplain surface following Midgley et al. (2012): that layer was given a thickness of 0.1 m, typical for the rooting depth of grass, a τ_c of 500 kPa, and a k_d of 0.004 $cm^3\ N^{-1}s^{-1}$.

Root Cohesion

The increased cohesion provided by the presence of roots, termed "root cohesion" (c_r, kPa) is incorporated into the modified Mohr-Coulomb equation as an additive factor:

$$s_r = c' + c_r + \sigma \tan(\phi') + \psi \tan(\phi^b) \quad (12)$$

The Bank Stability and Toe Erosion Model (BSTEM) includes a module "RipRoot" (Pollen-Bankhead and Simon, 2009) designed to calculate c_r by estimating both the rate of root breakage and root pull-out along the failure plane, and also the distribution of roots vertically through the soil profile. RipRoot includes a database of several common riparian plant species, and RipRoot users need only select the species, plant age, and percent of the total riparian assemblage to calculate the c_r. The RipRoot plant database includes only four species found at the study sites (River Birch, Cottonwood, Sycamore and Black Willow), and there is a poor correlation between DBH and plant age, so data collected in the field could not be directly incorporated into RipRoot. For the purpose of this study a relationship was developed between the estimated BGB and modeled RipRoot assemblages based on the four riparian tree species and "bare earth". The c_r calculated with this relationship ranged between 0 and 6 kPa. Because plant roots are not uniformly distributed in the subsurface, RipRoot distributes the c_r vertically through the soil profile, with the most added strength within 0.3 m of the soil surface (Pollen-Bankhead and Simon, 2009)

Results and Discussion

Soil Chemistry

A total of 161 samples from 6 sites were collected from streambanks and processed for the study. The site average range for pH (7.2-6.2) and EC (20.5-33.6 μS/cm) for samples were within the ranges expected for silt and silt-loam soils without excessive fertilizer application (Table 2).

Table 2. Average pH and electrical conductivity (EC, µS/cm) for soil samples by site.

	pH			EC	
Site	Mean	Standard Deviation	Description	Mean	Standard Deviation
A	7.20	0.26	Slightly basic	33.54	24.68
B	6.94	0.33	Slightly acid	23.51	10.29
C	6.54	0.29	Slightly acid	23.42	21.83
D	6.33	0.27	Slightly acid	34.34	31.26
E	6.41	0.34	Slightly acid	36.64	26.27
F	6.18	0.35	Slightly acid	20.48	14.63

Soil Phosphorus

The spatial distribution of sampling was designed to estimate the distribution P vertically below the surface at the face of the bank and horizontally into the bank. The mobility of P is a complex phenomenon, related to many factors, including soil texture and the chemistry of both the soil and water. To fully understand the importance of the P concentrations found at the sites, three different metrics from each sample were measured. These measurements are described fully in the methods section, and are briefly recapped below:

1. Water Soluble Phosphorus (WSP): This value is correlated to the amount of P that would be released from the soil to the stream. It is measured by suspending a known mass of sample in de-ionized water, agitating the mixture for a set time then filtering and measuring the P concentration in the water.
2. Degree of Phosphorus Saturation (DPS): This value estimates the likelihood of P mobility by reporting the concentration of P relative to the concentrations of the iron (Fe) and aluminum (Al) oxides that typically serve to bind P in soil. DPS is reported as a percentage, and values over 25% are often regarded as more likely to release P.
3. Total P (TP): This is a measure of all of the forms of P in the soil, is a common measurement that allows comparison to other studies and helps assess the potential for P desorbing from soil particles into water bodies under conditions not addressed by the WSP and DPS tests.

The P data for each site were displayed as an interpolated map representing the average distribution for each P metric within the streambank. The floodplain surface is the top of the map, and the streambank edge is at the left of the map. The range of concentrations represented by the contours varies by site and by P metric.

Site A

This unprotected site has high concentrations of all P metrics, especially at the floodplain surface (Figure 11); this reflects the site land use history, which includes row cropping and application of poultry litter. High WSP and DPS at the land surface indicate that surface runoff containing eroded soil may introduce P to the stream. The map of TP shows similar high concentrations at the floodplain surface, but also relatively high concentrations at the cohesive soil/gravel interface, indicating that some

P may have been transported into the floodplain by floodwater, where it became strongly bound to the cohesive soil. Similarly, an area of high TP is shown at the bank face.

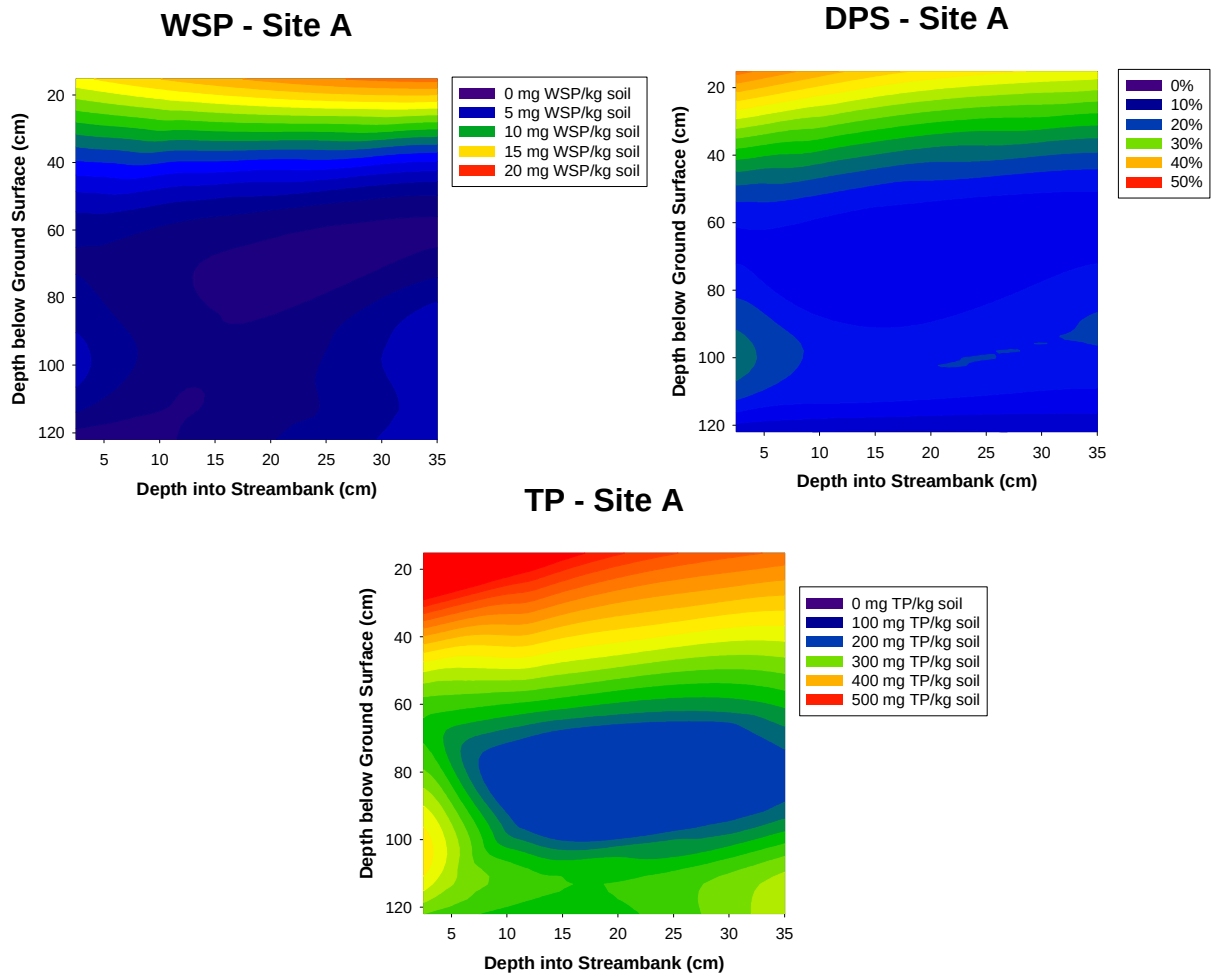

Figure 11. Spatial distribution of P within streambank soils at Site A.

Site B

This “protected” site has much lower concentrations of WSP and DPS at the floodplain surface, although the TP map shows a pattern similar to Site A (Figure 12).

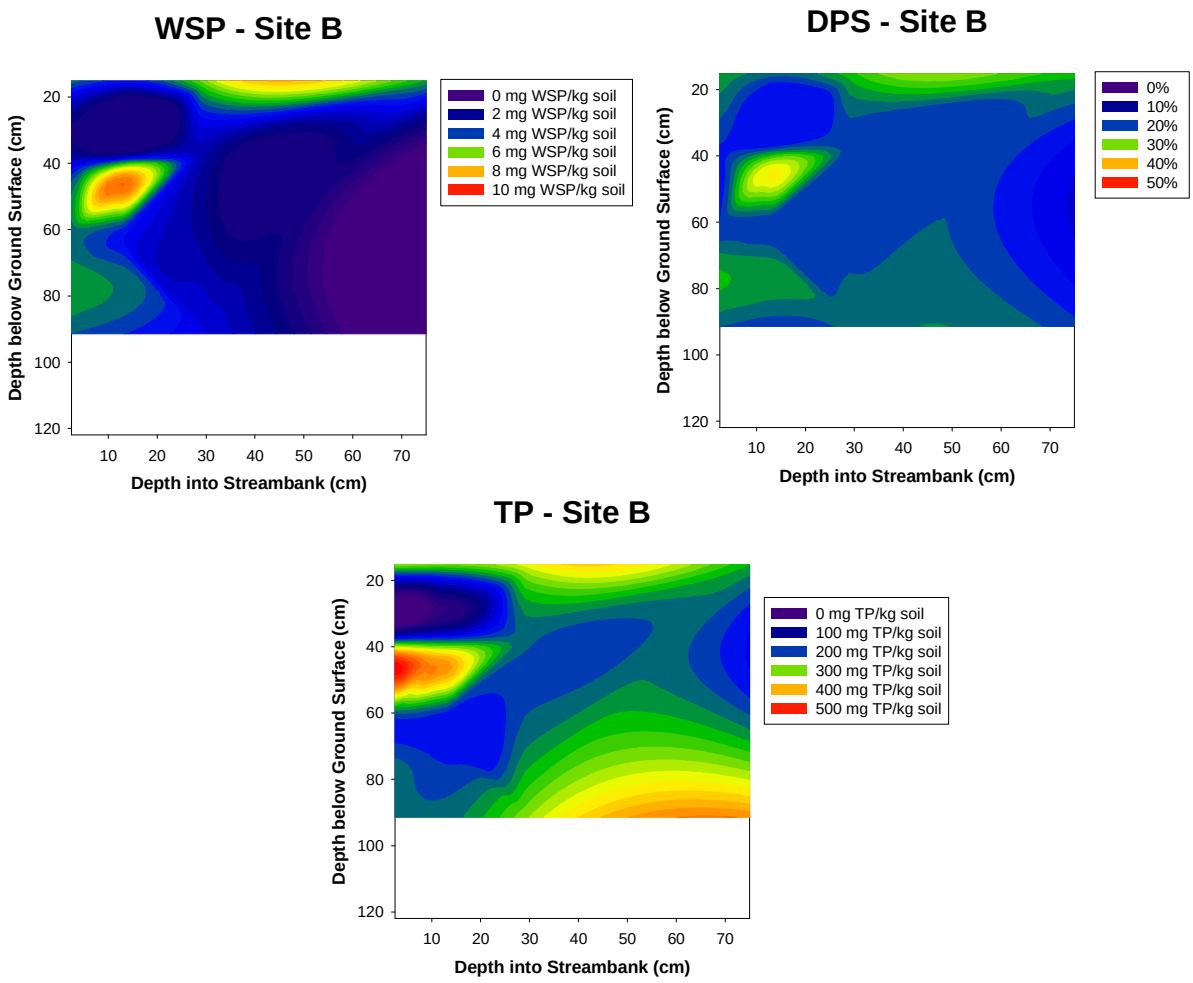

Figure 12. Spatial distribution of P within streambank soils at Site B.

Site C

This site shows low concentrations of P in streambank soils (Figure 13). Note that the map scale for the WSP concentrations is one-half that of Site B and one-fourth that of Site A. Interestingly, the DPS at Site C, which estimates the potential mobility of P by comparing P concentration to typical bonding sites, shows relatively high values, which may indicate significant variability in soil types throughout the watershed. The distribution of TP is similar to that seen in Sites A and B, showing significant TP concentrations at the soil/gravel interface, and along the bank face.

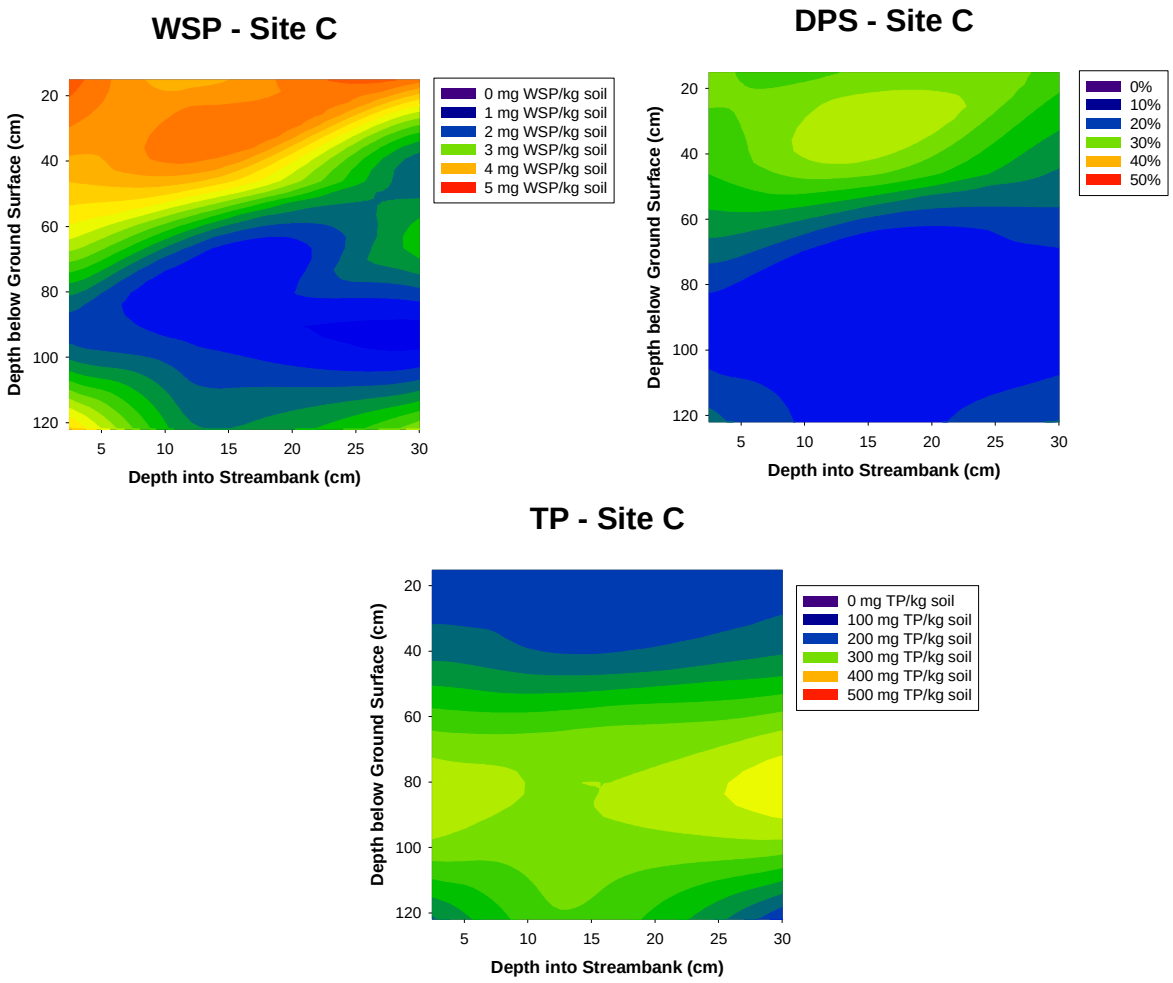

Figure 13. Spatial distribution of P within streambank soils at Site C.

Site D

This "protected" site shows a different spatial distribution of P within the streambank (Figure 14). The WSP is highest near the floodplain surface as is common; however, in contrast to the other sites, DPS is uniform throughout the sampling area and extremely low. Similar to DPS, TP is distributed uniformly throughout the floodplain soil but is relatively high.

Site E

This "unprotected" site shows a spatial distribution of P largely similar to that of Site D (Figure 15). The maps show low and uniform DPS, high and uniform TP, but the WSP distribution is low everywhere except at a single location along the bank face.

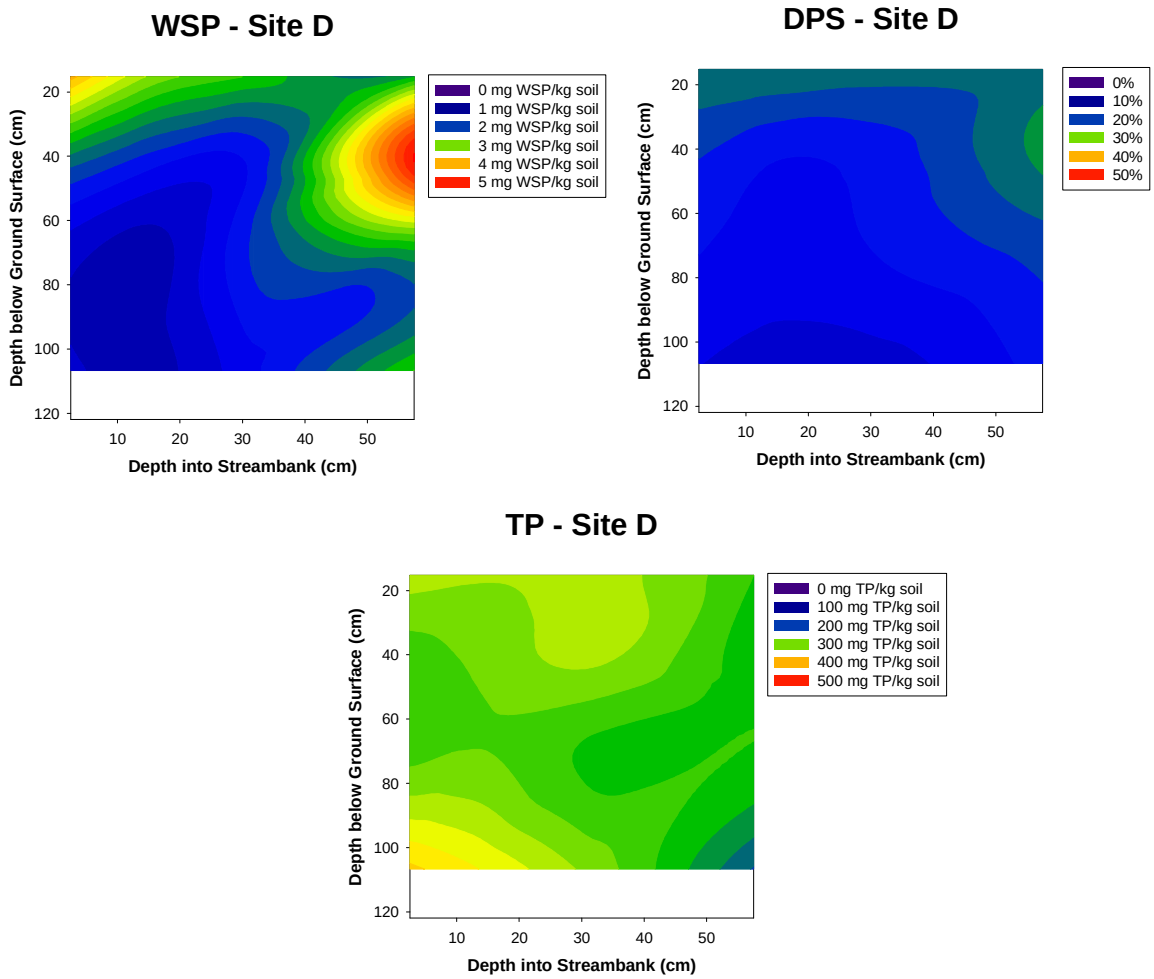

Figure 14. Spatial distribution of P within streambank soils at Site D.

Site F

This unprotected site shows a P spatial distribution that is again similar to Sites D and E, with low and uniform DPS and high and relatively uniform TP, but WSP at the site is only found at the soil/gravel interface (Figure 16).

Environmentally Sensitive P Concentrations

It is recognized that excess P represents a threat to the quality of fresh water, and that soil is a potential non-point source of P. The variability inherent in soils affects the release of soil-bound P into the environment, and the soil P metrics (WSP and DPS) have each been used to estimate the potential for that release. Soils with DPS values greater than a threshold of 25% and/or greater than 8.2 mg WSP kg^{-1} have commonly been assumed to indicate the potential to release P into water (Figure 17). The environmental thresholds divide Figure 17 into four quadrants: samples in the lower left

are below both the DPS and WSP thresholds; those in the upper left are above the DPS but below the WSP thresholds; in the lower right are the samples below DPS but above WSP; and in the upper right are those above both the DPS and WSP thresholds. It is apparent from the plot in Figure 17 that the DSP and WSP metrics do not identify all of the same samples as being potentially environmentally damaging. It was beyond the scope of this project to identify which P metric was most appropriate for identifying environmentally sensitive P concentrations, but it is obvious that a significant number of randomly-selected bank samples are likely to contain environmentally sensitive concentrations of P that should be considered likely to readily enter the stream water in the event of bank erosion.

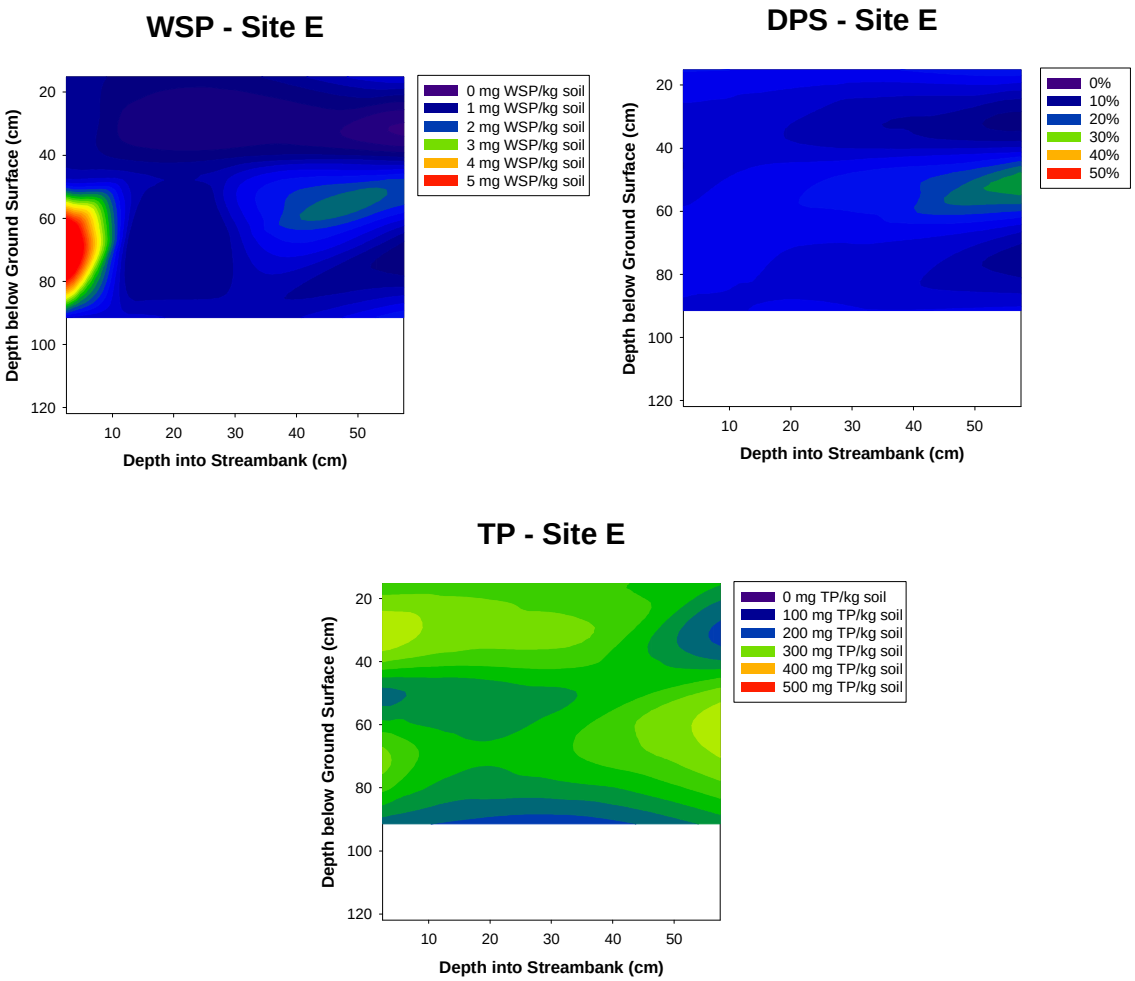

Figure 15. Spatial distribution of P within streambank soils at Site E.

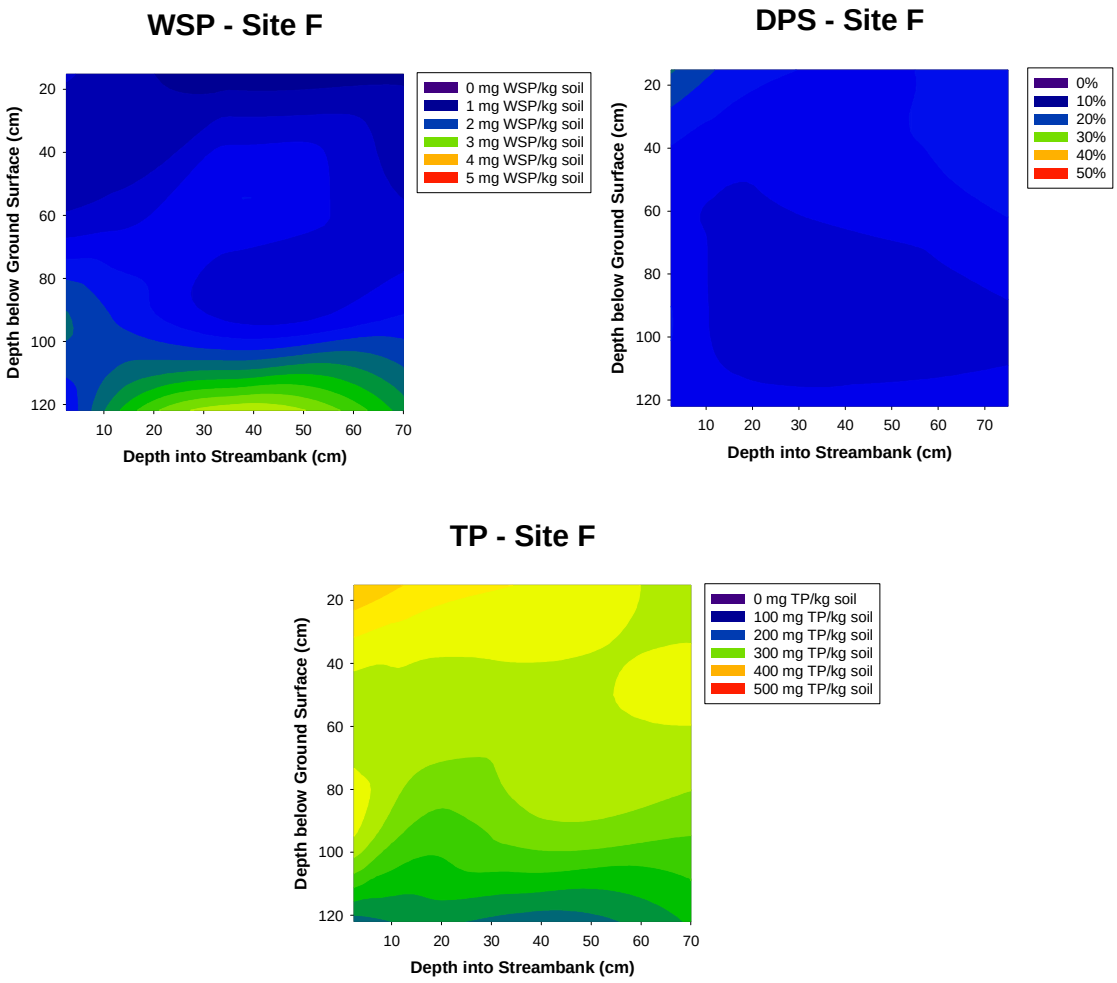

Figure 16. Spatial distribution of P within streambank soils at Site F.

P Loading

A total mass of eroded soil per site was calculated using equation (3), and using the average WSP and TP from samples for all six sites, WSP and TP loads were estimated (Table 3). In total those 6 sites contributed a total of 173 kg of WSP and 14880 kg TP to the Barren Fork Creek over the seven year study period. Across the sites, the average WSP load was 30 kg in seven years or 4.3 kg WSP/yr, and the TP load was 2500 kg or 355 kg TP/yr. The WSP loading was dominated by erosion at the unprotected sites where the total over the seven years was 50.1 kg WSP (7.2 kg WSP/yr), whereas the protected sites had an average WSP contribution of 9.9 kg in seven years (1.4 kg WSP/yr). In contrast, TP loading was similar between all sites, with the 307 kg TP (43.8 kg TP/yr) average for unprotected sites similar to 259 kg TP (36.9 kg TP/yr) for protected sites.

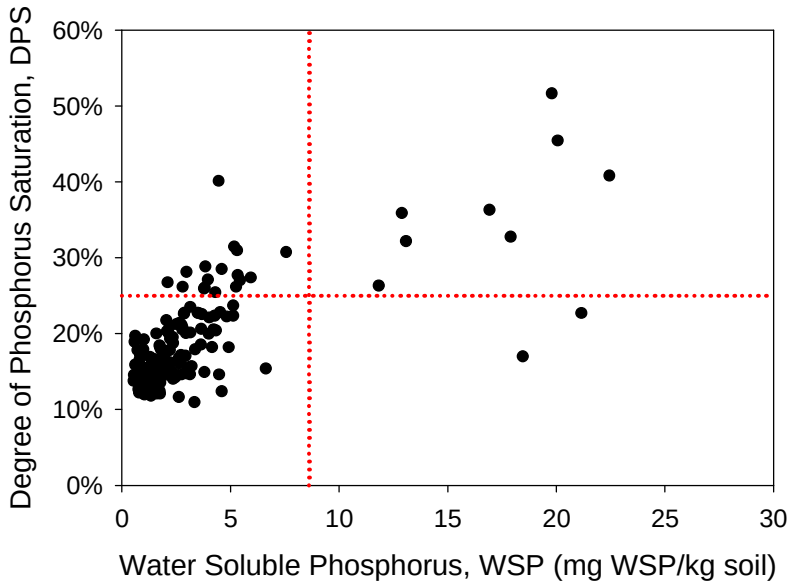

Figure 17. Environmental sensitivity of streambank soil samples. The dashed red lines represent accepted threshold concentrations: 8.2 mg WSP kg^{-1} and 25% DPS.

The reach-averaged contributed WSP across all sites was 22 g WSP/yr/m of bank. The average for unprotected sites was 37 g WSP/yr/m of bank while that for protected sites was 8 g WSP/yr/m of bank. While these values appear very different, a two-sample T-test for differences of means was not significant ($P = 0.23$, $\alpha = 0.05$) because of the small sample size, and also because the high average for protected sites was driven by the high value for Site A (Table 3). Despite similar TP concentrations in the soils across sites, reach-averaged TP loads were different because of the difference in eroded area: unprotected 3415 kg/m/yr and protected 622 kg/m/yr, which was statistically significant ($P = 0.008$, $\alpha = 0.05$). Note that these P loading rates were dependent on how representative the sampled streambanks are relative to the rest of the watershed, and more data should be collected to verify these initial findings.

The WSP and TP loading rates can be used in conjunction with the helicopter video survey of bank stability to estimate a watershed-scale load. The stability of Barren Fork Creek streambanks as a percent of each 2 km reach of both left and right banks is shown in Figure 18. The entire stream length (~55 km) within Oklahoma was surveyed. The failure percentage per 2 km reaches ranges from 11 to 55% with an average value of 36%, meaning that more than one-third of the length of Barren Fork Creek has unstable and eroding banks. Annual WSP loading from the Barren Fork from unprotected and failing streambanks, calculated by multiplying the failing length of Barren Fork Creek by the averages of WSP and TP per meter of bank, was 1540 kg WSP/yr and 79,930 kg TP/yr.

Table 3. Volume and mass of eroded soil, and WSP and TP loading for study sites. WSP and TP values are shown both as site totals and as reach-length-averaged annual loads.

	Unprotected			Protected		
	A	E	F	B	C	D
Total Soil Volume Eroded[a] (m^3 x 10^3)	10.2	11.4	6.1	1.7	2.5	1.6
Total Soil Mass Eroded (kg x 10^6)	15.4	17.1	9.1	2.5	3.8	2.4
Average WSP (mg P/kg soil)	7.2	1.2	1.4	3.9	3.2	2.4
Total Contributed WSP (kg P)	111	21	13	10	12	6
Contributed WSP/yr/m (g/m/yr)	83	16	12	6	13	5
Average TP (mg P/kg soil)	360	250	311	250	240	286
Total Contributed TP (kg P)	5541	4283	2832	625	913	687
Contributed TP/yr/m (g/m/yr)	4166	3307	2771	383	945	539

[a] Eroded Area (m^2) x Soil Depth (m) from Table 1

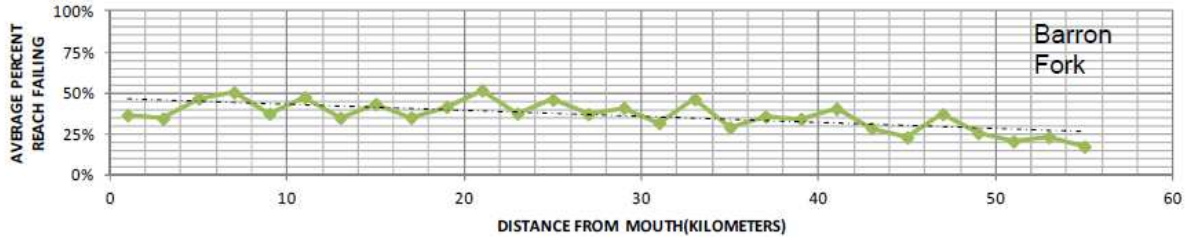

Figure 18. Results of helicopter-borne video survey of Barren Fork Creek streambanks. The vertical scale of the plot refers to the percent of the total bank length (both left and right) that was classified as "failing" for each 2 km reach.

LOADEST

The LOADEST estimates from the Eldon gauge were generally better than those from the Dutch Mills gauge, based on the Nash-Sutcliffe Model Efficiency (NSE) value (Table 4), with the dissolved P estimate performing better than TP. Plots of observed versus modeled TP and dissolved P confirms that the Eldon LOADEST model fit observed data much better than the Dutch Mills model (Figure 19). According to Figures 19a and 19b, the Dutch Mills model under predicted the TP and dissolved P loads.

The calculated average of the LOADEST dissolved P estimate for the Barren Fork Creek from 2003-2010 was 13,833 kg/yr; thus streambank WSP likely contributed more than 10% of that estimated load. The LOADEST TP annual average load was 46,416 kg/yr, which was less than the 79,930 kg TP/yr estimated from streambanks in this study. However, unlike WSP, which is dissolved and thus will travel within the water column, TP is largely a sediment-bound constituent, and thus is subject to sediment transport dynamics. It is unlikely that all of the bank sediment that is eroded into the

stream will be retained and transported within the stream to its outlet. Instead, some portion will be deposited some shorter distance downstream as point bar or overbank material. It is thus not surprising that the TP within the eroded bank material is greater than the TP estimated from the USGS gauge data; that TP likely is dominated by bank and surface erosion from an area relatively close to the gauge.

Table 4. LOADEST model fit statistics for the USGS gauges at Dutch Mills, AR and Eldon, OK. Shown are coefficient of determination (R2) and Nash-Sutcliffe Model Efficiency (NSE) for the observed and LOADEST-predicted P species at the respective gauges for the period 2003-2010.

	Fit Statistic	Total Phosphorus (mg/L)	Dissolved Phosphorus (mg/L)
Barren Fork Creek at Dutch Mills, AR	R^2	0.14	0.08
	NSE[1]	0.12	0.03
Barren Fork Creek at Eldon, OK	R^2	0.66	0.84
	NSE	0.54	0.82

BSTEM

Calibration of the BSTEM models was achieved by manipulating α, τ_c, and k_d (Table 5). There was generally good agreement between the total retreat predicted by the calibrated BSTEM models for each site and the *SR* measured from NAIP aerial imagery (Figure 20). The comparison between the interim time intervals (2003-2008, 2008-2010) shows that the 'protected site" (B, C, and D) BSTEM retreat predictions agree much more closely with *SR* than the "unprotected", with the model over-predicting retreat 2003-2008 and under-predicting 2008-2010 (Figure 20). This disparity may be partially explained by observing that the sites with the greatest difference between measured and modeled bank retreat were ones with the most bank erosion. At those sites (A, E, and F) it is likely that the conditions affecting bank erosion changed over the course of the study period, most notably the ROC (Figure 4, Figure 8, and Figure 9). BSTEM models the streambank as a straight reach of infinite length, so the important erosive characteristics typical of curvature at a site were modeled by applying a uniform α to the τ_c and k_d. The sites with the most change in ROC will have the highest standard deviation of ROC (ROC_{SD}). A plot of α and ROC_{SD} shows that the highest α corresponds to the lowest ROC_{SD} and the largest *SR* (Figure 21).

This makes intuitive sense; a high ROC_{SD} implies that the ROC and hence the erosive characteristics of the curve also changed dramatically at the site; in contrast, the α used in BSTEM to simulate those erosive characteristics was constant over the modeling period. Therefore, predictions of the timing of bank retreat were likely affected, and especially at sites with the highest ROC_{SD}.

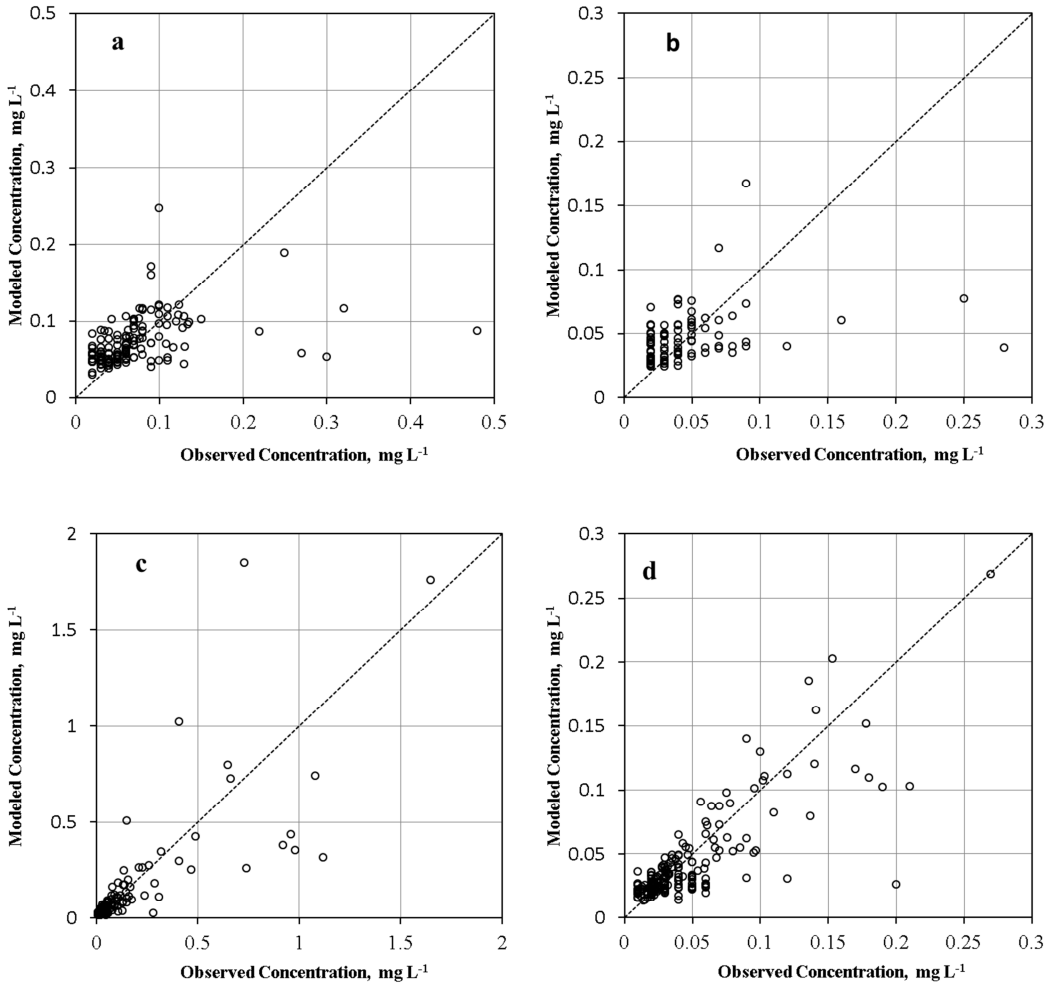

Figure 19. Plots of observed and LOADEST predicted concentrations for TP at Dutch Mills (a) and Eldon (c), and Dissolved P at Dutch Mills (b) and Eldon (d).

Root Cohesion

The effect of c_r on bank retreat was evaluated by increasing the c_r in the calibrated "unprotected" sites (A, E, and F). While c_r had no significant effect on the large amounts of bank retreat evident at those sites, increasing the c_r did seem to affect the variability of retreat. Because c_r adds to soil strength, increasing c_r may either allow the cohesive soils to form an overhanging shelf as the gravel layer is eroded away, or allow larger soil blocks to fail. Multiple regression of τ_c, k_d and c_r against bank retreat (m) was used to determine which BSTEM model inputs significantly affected bank retreat. It was found that only k_d was a significant predictor ($\alpha = 0.05$). The sites B, C and D had riparian forest along the bank. The BSTEM calibrations for those sites included both adding c_r and decreasing the initial k_d, which suggested that tree roots not only affected soil strength, but also affected soil erodibility. The effect of plant roots on soil erodibility has been addressed, but no predictive relationships exist that can be used in BSTEM.

Table 5. Calibrated and original (base case) BSTEM model parameter values for sites. ϕ' is internal angle of friction, c' is apparent cohesion, S_w is saturated weight of soil, τ_c is critical shear stress, k_d is soil erodibility, and c_r is root cohesion.

	Site	Material	ϕ' (°)	c' (kPa)	S_w (kN/m^3)	τ_c (Pa)	k_d (cm^3/Ns)	α	Bank Height (m)	Soil Depth (m)	Root Depth (m)	c_r (kPa)
A	Calibrated	Soil	31.8	2.96	18.0	0.84	10.00	1.2	2.80	1.58	*	*
		Gravel	31	0	20.0	2.89	1.44					
A	Base Case	Soil	31.8	2.96	18.0	1.01	660.00	1	2.80	1.58	*	*
		Gravel	31	0	20.0	3.47	1.20					
B	Calibrated	Soil	35.9	4.97	18.0	3.92	8.12	1	2.72	0.93	0.90	1.50
		Gravel	34.8	0	20.0	5.50	0.95					
B	Base Case	Soil	35.9	4.97	18.0	2.38	35.50	1	2.72	0.93	0.90	1.50
		Gravel	34.8	0	20.0	5.50	0.95					
C	Calibrated	Soil	38.2	2.91	18.0	2.79	5.30	1	4.57	2.16	1.00	3.40
		Gravel	33.9	0	20.0	6.98	0.84					
C	Base Case	Soil	38.2	2.91	18.0	2.79	7.30	1	4.57	2.16	1.00	3.40
		Gravel	33.9	0	20.0	6.98	0.84					
D	Calibrated	Soil	26	6.34	18.6	5.50	5.40	1	2.25	0.59	0.58	6.80
		Gravel	32	0	20.0	6.07	0.90					
D	Base Case	Soil	26	6.34	18.6	0.75	148.87	1	2.25	0.59	0.58	6.03
		Gravel	32	0	20.0	6.07	0.90					
E	Calibrated	Soil	26	6.34	18.1	0.80	50.00	3	2.88	0.77	*	*
		Gravel	32.1	0	20.0	1.47	3.18					
E	Base Case	Soil	26	6.34	18.1	2.39	53.61	1	2.88	0.77	*	*
		Gravel	32.1	0	20.0	4.40	1.06					
F	Calibrated	Soil	31.8	2.96	18.0	1.04	10.00	1.35	3.15	0.74	*	*
		Gravel	31	0	20.0	6.44	1.08					
F	Base Case	Soil	31.8	2.96	18.0	1.40	121.90	1	3.15	0.74	*	*
		Gravel	31	0	20.0	8.70	0.80					

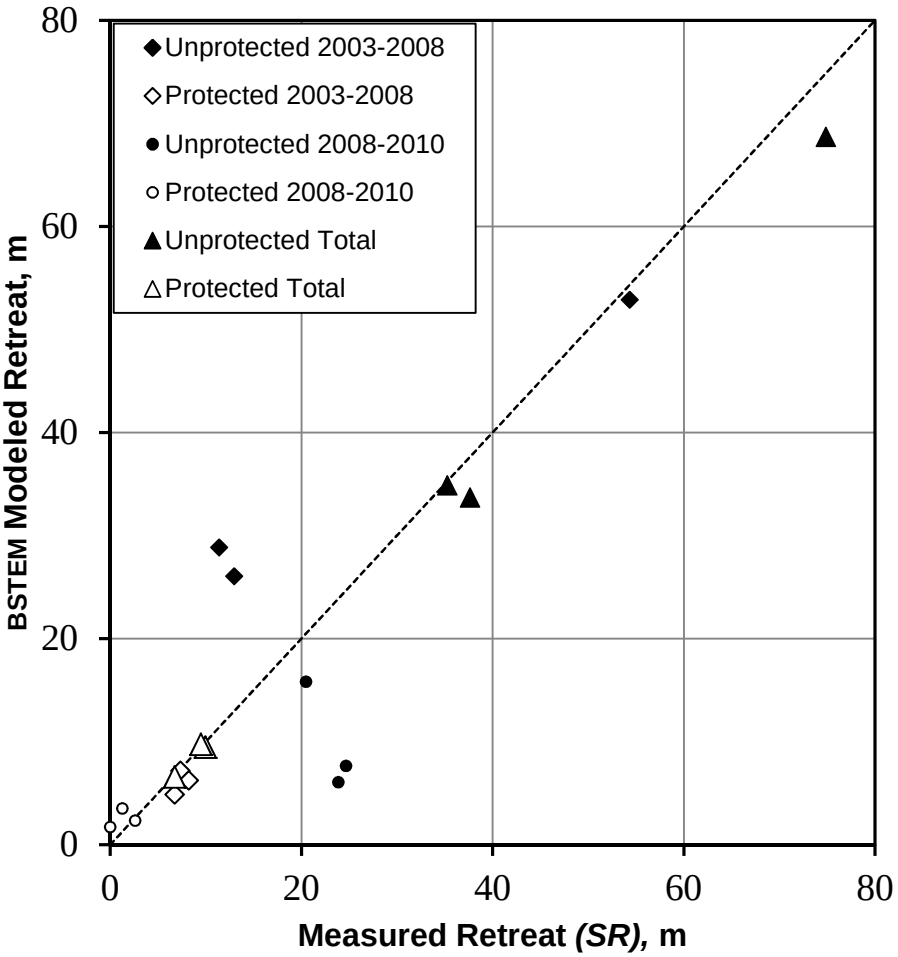

Figure 20. Comparison of measured bank retreat (*SR*) from aerial imagery to predicted retreat estimates from BSTEM. Perfect agreement is shown as the dashed line.

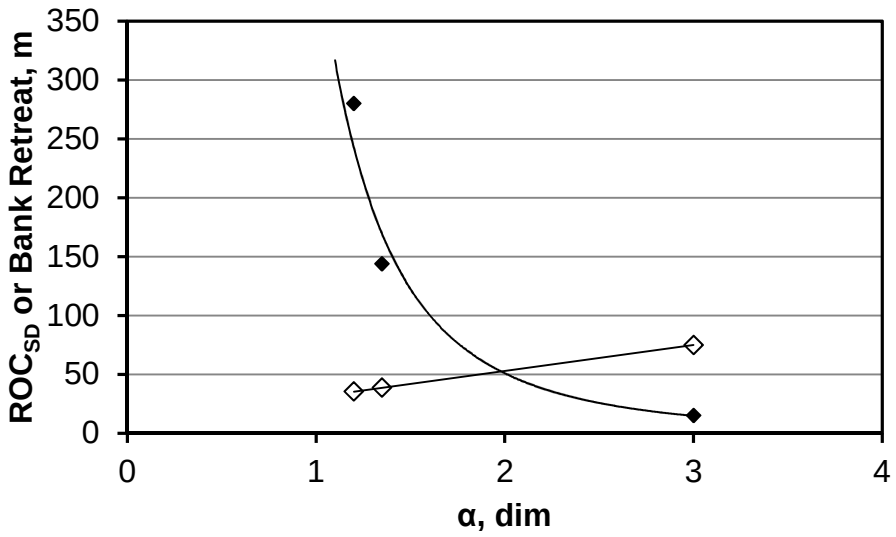

Figure 21. BSTEM *α* calibration factor (dimensionless), which simulates stream curvature, and the standard deviation of radius of curvature (ROC_{SD}, solid symbol) estimated from aerial imagery, and BSTEM modeled bank retreat (hollow symbol).

Flood Event Erosion Characteristics

The calibrated BSTEM models were used to investigate the effect of flood event characteristics, particularly multiple event peaks and event magnitude, on bank retreat at the sites. A major single-peak flood event (2011 event, 4/13/2011 to 5/13/2011) and a multiple peak event (4/4/2013 to 6/6/2013) were chosen and modeled with the calibrated BSTEM parameters. The unprotected sites showed much more bank retreat than the protected sites, with the multiple-peak event producing no bank top retreat at the protected sites (Table 6). The bank top retreat for the 2011 event appeared to occur mainly on the falling limb of the hydrograph (Figure 22), a typical time for bank failure because the cohesive layer was the heaviest because it was still saturated but the support provided by the high stream stage was no longer present. Similarly, the multiple peak event bank top retreat occurred with the onset of the falling limb (Figure 23); however, except for Site A, the retreat was concentrated at the falling of the third peak. The final bank profile at Site B (Figure 24) and also at Sites C and D showed no bank top retreat, but there was nonetheless noticeable fluvial erosion within the gravel layer. It seemed apt to assume that fluvial erosion of the gravel layers occurred with each peak, but that only after the third peak was the bank unstable enough to cause a failure and bank retreat.

Table 6. Modeled bank top retreat at study sites for major single-peak flood event (4/13/2011 to 5/13/2011) and a multiple peak event (4/4/2013 to 6/6/2013).

		Bank Retreat (m)	
		Single 2011	Multiple 2013
Unprotected	A	12.9	2.8
	E	17.8	1.2
	F	5.3	1.0
Protected	B	2.3	0.0
	C	3.9	0.0
	D	2.6	0.0

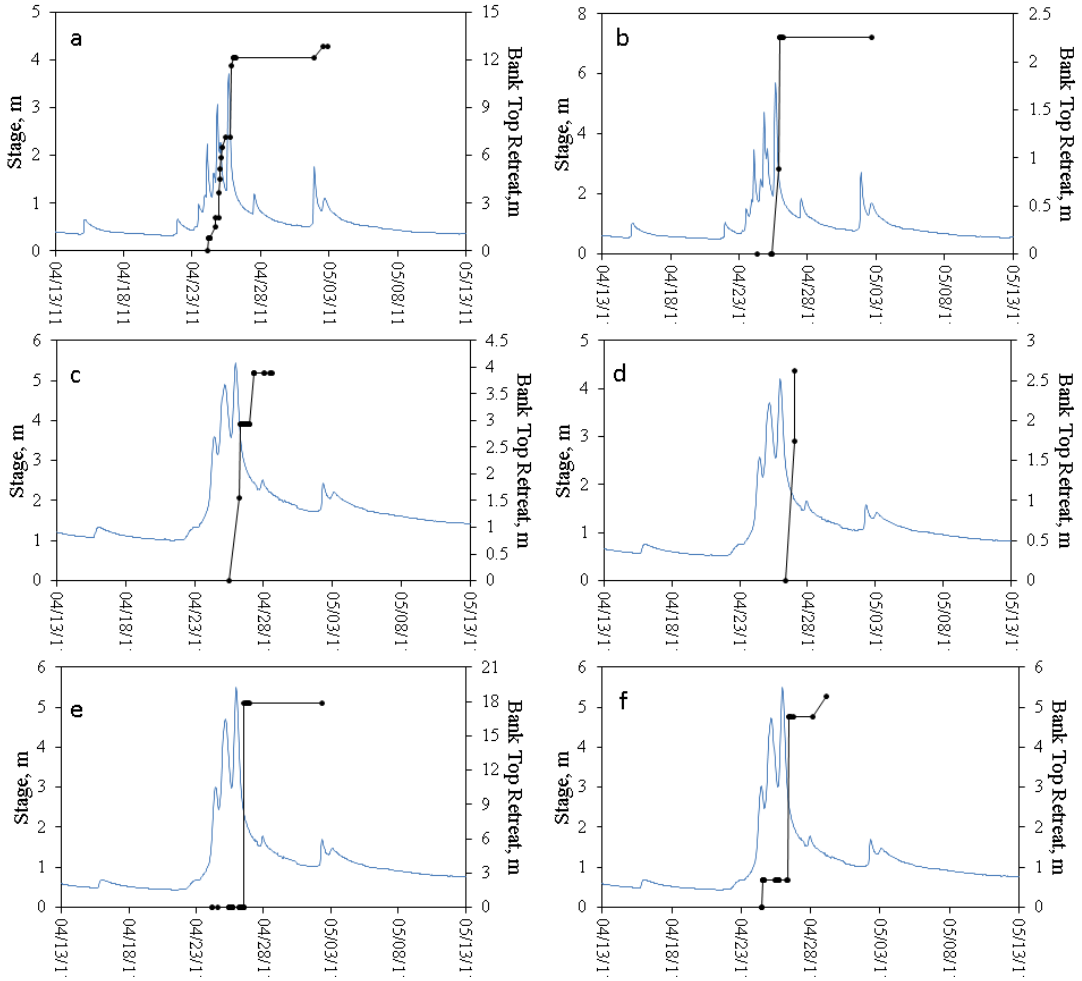

Figure 22. Stream stage hydrograph and bank retreat timing for 2011 flood event (4/13/2011 to 5/13/2011) for Site A (a), Site B (b), Site C (c), Site D (d), Site E (e), and Site F (f).

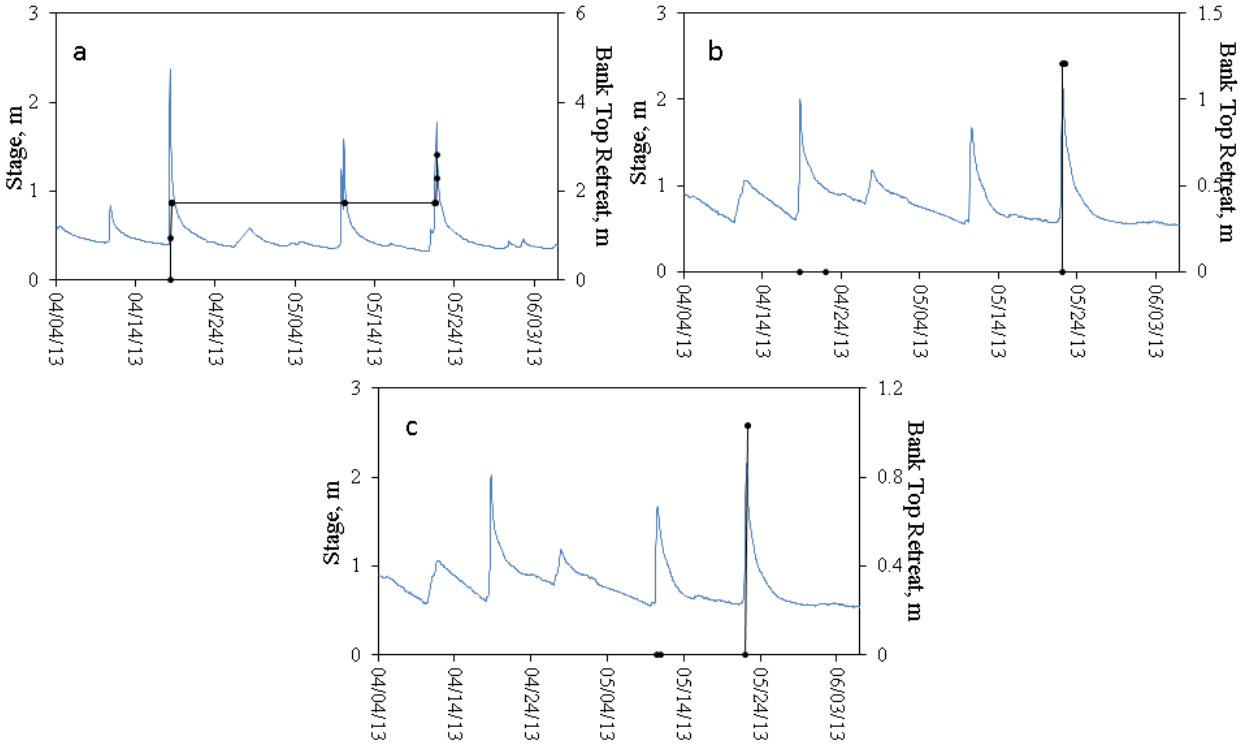

Figure 23. Stream stage hydrograph and bank retreat timing for 2013 multiple peak flood event (4/13/2011 to 5/13/2011) for Site A (a), Site E (b), and Site F (c).

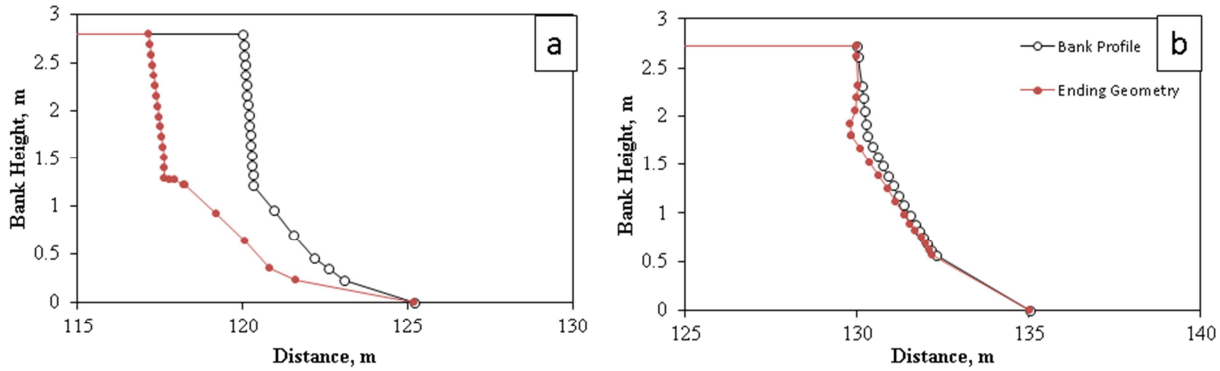

Figure 24. Initial and final bank profiles for BSTEM model of multiple peak flood event (4/13/2011 to 5/13/2011) for Site A (a) and Site B (b). Significant bank top retreat is evident at Site A, likely a combination of fluvial erosion and geotechnical failure, while Site B shows only fluvial erosion within the gravel layer.

Field Monitoring of Streambank Erosion Rates

Field measurement of streambank erosion can be a time-consuming and labor-intensive process, requiring repeated surveys utilizing permanent survey monuments or monitoring bank erosion pins. Both of these methods require the time of trained personnel over a period encompassing one or more years to assess the rate of erosion. Since bank erosion is linked to stream flow, and stream flow varies over time, shorter monitoring periods are likely to be much more variable in assessing bank erosion, with a particular period likely to over- or under-estimate the rate of erosion. To test this, the BSTEM modeled bank retreat over the 7-yr study period, which included water years both above and below the average flow, was divided into 1-, 2-, and 3-yr intervals and the BSTEM bank retreat totaled for those periods.

As might be expected, a 1-yr monitoring period was highly variable for both "unprotected" (Figure 25) and "protected" sites (Figure 26), with some "protected" sites having no erosion for 1 or more years. Erosion at the "unprotected" sites was detected for each 1-yr period, but the rates varied, with some yearly rates as high as 25 m/yr (Figure 25b). The 3-yr monitoring intervals were more consistent; however, there is a loss in resolution as the higher erosion rates are gradually averaged out over a longer period of time. For example, for the "unprotected" sites (Figure 25), a one year monitoring record could produce a maximum retreat rate of nearly 25 m/yr at Site E while a 3-yr monitoring record may only show a maximum retreat of less than 15 m/yr.

Also, the period in which monitoring takes place can make a drastic difference on estimated annual bank retreats. For example, if a 2-yr monitoring period was chosen to estimate the annual average retreat for Site A, the estimates would be radically different if that survey was taken in 2004-2005 as opposed to 2006-2007. Estimates for a 2-yr monitoring period for 2004-2005 would be approximately 9 m/yr of bank retreat while estimates for 2006-2007 would be approximately 1 m/yr of bank retreat.

These comparisons (Figure 25 and 26) illustrate the episodic nature of streambank erosion and bank retreat. Long-term monitoring may not capture the active years of bank erosion while short-term monitoring may miss erosion events altogether. Because of this, there is a great need for the use of bank stability models such as BSTEM that use physical processes based on site characteristics to incrementally model bank retreat for longer periods of time. This will provide a better set of tools for watershed managers to use when making management decisions associated with site stability or sediment and nutrient loading.

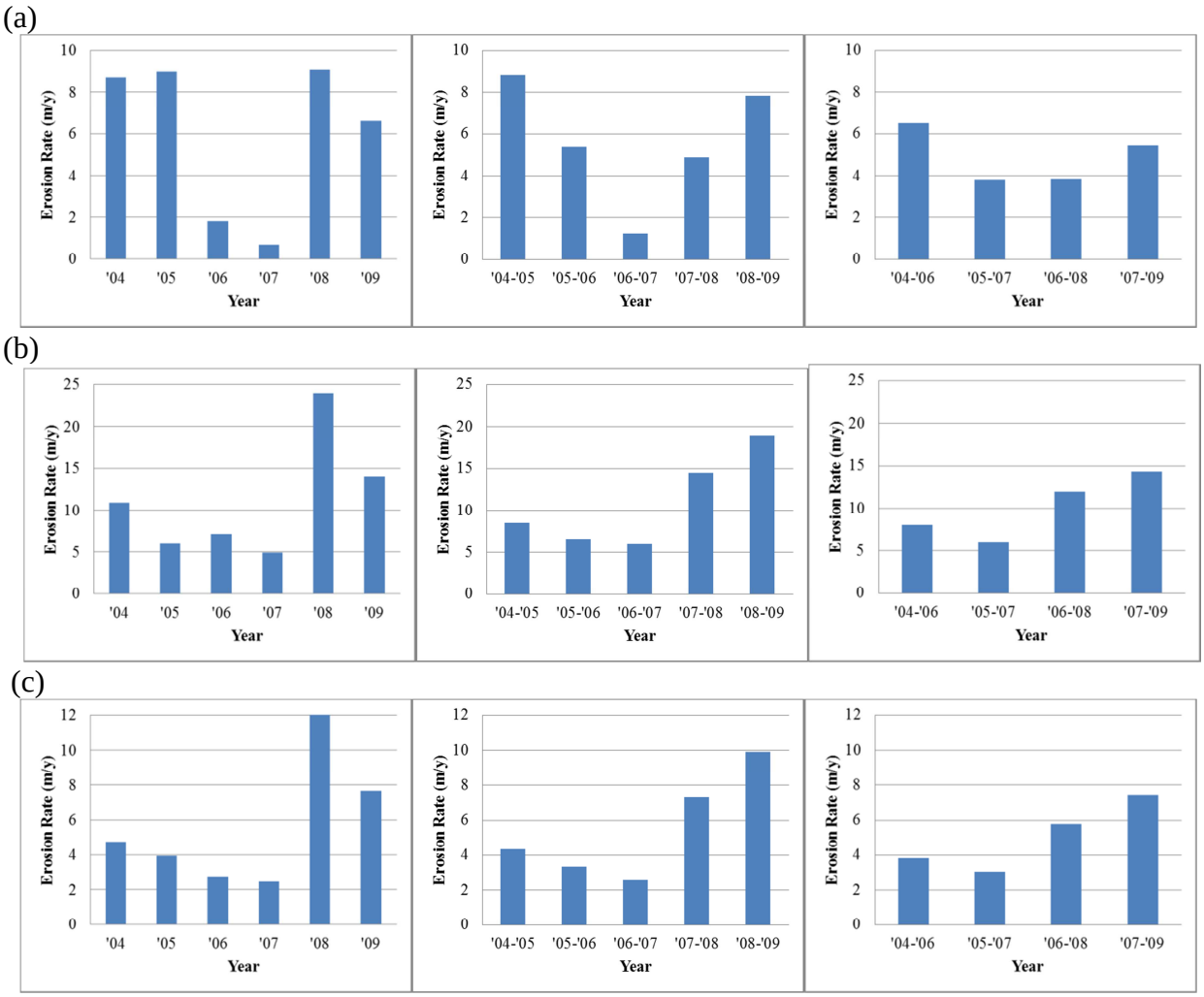

Figure 25. Erosion rates averaged over 1, 2, and 3 yrs (from left to right respectively) at the "unprotected" (a) site A, (b) site E, and (c) site F.

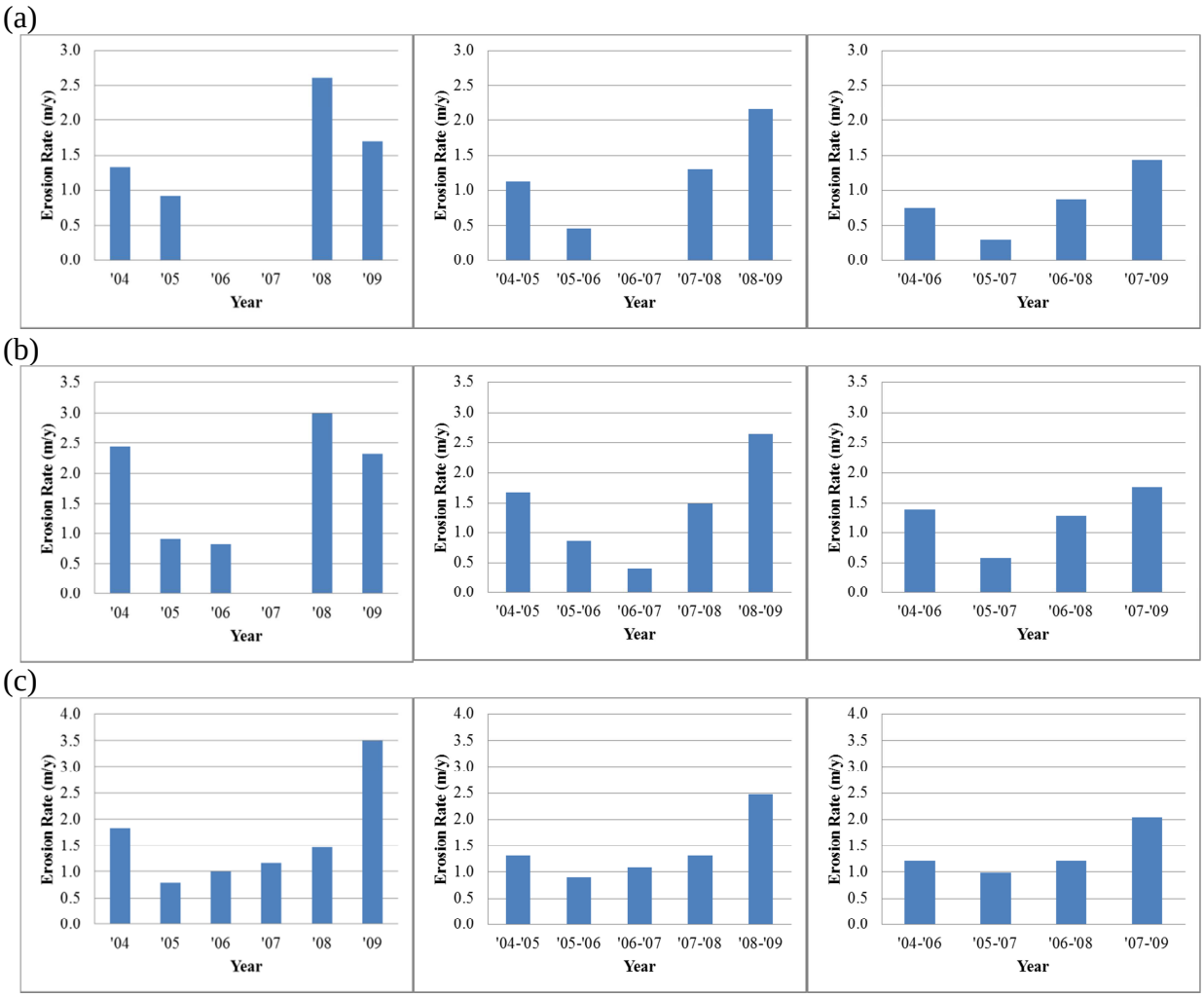

Figure 26. Erosion rates averaged over 1, 2, and 3 yrs (from left to right respectively) at the "protected" (a) site B, (b) site C, and (c) site D.

Literature Cited

Al-Madhhachi, A. T., G. J. Hanson, G. A. Fox, A. K. Tyagi, and R. Bulut. 2013. Deriving parameters of a fundamental detachment model for cohesive soils from flume and jet erosion tests. *T. ASABE* 56(2): 489-504.

Bernhardt, E. S., M. A. Palmer, J. D. Allan, G. Alexander, K. Barnas, S. Brooks, J. Carr, S. Clayton, C. Dahm, J. Follstad-Shah, D. Galat, S. Gloss, P. Goodwin, D. Hart, B. Hassett, R. Jenkinson, S. Katz, G. M. Kondolf, P. S. Lake, R. Lave, J.L. Meyer, T. K. O'Donnell, L. Pagano, B. Powell, and E. Sudduth. 2005. Synthesizing U.S. river restoration efforts. *Science* 308: 636-637, DOI:10.1126/science.1109769.

Crosato, A. 2007. Physical explanations of variations in river meander migration rates from model comparison. *Earth Surf. Proc. Land.* 34: 2078-2086.

Crosta, G., and C. di Prisco. 1999. On slope instability induced by seepage erosion. *Can. J. Geotech.* 36: 1056-1073.

Darby, S. E., and C. R. Thorne. 1996. Numerical simulation of widening and bed deformation of straight sand-bed rivers. I. Model development. *J. Hydraulic Eng.* 122: 184-193.

Darby, S. E., M. Rinaldi, and S. Dapporto. 2007. Coupled simulations of fluvial erosion and mass wasting for cohesive river banks. *J. Geophysical Res.* 112, F03022, doi: 10.1029/2006JF000722.

EPA. 2007. Method 3051a: Microwave-assisted acid digestion of sediments, sludges, soils and oils, Revision 1. Available online at: http://www.epa.gov/osw/hazard/testmethods/sw846/index.htm. Accessed 10/16/2013.

Fredlund, D. G., and H. Rahardjo. 1993. Soil Mechanics of Unsaturated Soils. New York, N.Y.: John Wiley and Sons, Inc.

Fuhrman, J. K., H, Zhang, J. L. Schroeder and R. L. Davis. 2005. Water soluble phosphorus as affected by soil to extractant ratios, extraction time and electrolyte. *Comm. Soil Sci. Plant Anal.* 36: 925-935.

Garcia, M., 2008. Sediment Transport and Morphodynamics. In Sedimentation Engineering: Processes, Measurements, Modeling and Practice, ASCE Manuals and Reports on Engineering Practice No. 110, 21-164. M. Garcia, ed. Reston, VA: American Society of Civil Engineers.

Hanson, G. J. 1990. Surface erodibility of earthen channels at high stresses: Developing an in situ testing device. *T. ASAE* 33(1): 132-137.

Hanson, G. J., and A. Simon. 2001. Erodiblity of cohesive sediment in the loess area of the Midwestern USA. *Hydrol. Proc.* 15: 23-28.

Heeren, D. M., A. R. Mittelstet, G. A. Fox, D. E. Storm, A.-S. Al-Madhhachi, T. L. Midgley, A. F. Stringer, K. B. Stunkel, and R. B. Tejral. 2012. Using rapid geomorphic assessments to assess streambank stability in Oklahoma Ozark streams. *T. ASABE* 55(3): 957-968.

Houben, D., C. Meunier, D. Periera and Ph. Sonnet. 2011. Predicting the degree of phosphorus saturation using the ammonium acetate-EDTA test. *Soil Use Manage.* 27: 283-293.

Jenkins, J. C., D. C. Chojnacky, L. S. Heath and R. A. Birdsey. 2004. Comprehensive database of diameter-based biomass regressions for North American tree species. USDA Northeastern Research Station. *General Technical Report NE-319*.

Krause, P., D. P. Boyle, and F. Base. 2005. Comparison of different efficiency criteria for hydrological model assessment. *Advances in Geosciences* 5: 89-97.

Kronvang, B., J. Audet, A. Baattrup-Pedersen, H. S. Jensen and S. E. Larsen. 2012. Phosphorus loads to surface water from bank erosion in a Danish lowland river basin. *J. Environ. Qual.* 41: 304-313.

Laubel, A., B. Kronvang, A. B. Hald and C. Jensen. 2003. Hydromorphological and biological factors influencing sediment and phosphorus loss via bank erosion in small lowland rural streams in Denmark. *Hydrol. Proc.* 17(17): 3443-3463.

Lavendel, B., 2002. The business of ecological restoration. *Ecol. Res.* 20: 173-178.

Mehlich, A. 1984. Mehlich 3 soil test extractant: A modification of the Mehlich-2 extractant. *Comm. Soil Sci. Plant Anal.* 15(12): 1409-1416.

Midgley, T., G.A. Fox, and D.M. Heeren. 2012. Evaluation of the Bank Stability and Toe Erosion Model (BSTEM) for predicting lateral streambank retreat on composite streambanks. *Geomorphology* 145-146: 107-114.

Mittelstet, A.R., D.M. Heeren, G.A. Fox, D.E. Storm, M.J. White, and R.B. Miller. 2011. Comparison of subsurface and surface runoff phosphorus transport rates in alluvial floodplains*. Ag. Ecosystems Environ*. 141: 417-425, DOI: 10.1016/j.agee.2011.04.006.

Murphy, J., and J. R. Riley. 1962. A modified single solution method for the determination of phosphate in natural waters. *Anal. Chim. Acta* 27: 31-36.

Papanicolaou, A. N., M. Elhakeem, and R. Hilldale. 2007. Secondary current effects on cohesive river bank erosion. *Water Resour. Res.* 43, W12418, doi: 10.1029/2006WR005763.

Partheniades, E. 1965. Erosion and deposition of cohesive soils. *J. Hydraulics Div. ASCE* 91(HY1): 105-139.

Pizzuto, J. E. 2008. Streambank Erosion and River Width Adjustment. In Sedimentation Engineering: Processes, Measurements, Modeling and Practice, ASCE Manuals and Reports on Engineering Practice No. 110, 387-438. M. Garcia, ed. Reston, VA: American Society of Civil Engineers.

Pollen-Bankhead, N. and A. Simon. 2009. Advanced application of root-reinforcement algorithms for bank stability modeling. *Earth Surf. Proc. Land.* 34: 471-480.

Pote, D.H., T.C. Daniel, A.N. Sharpley, P.A. Moore, Jr., D.R. Edwards, and D.J. Nichols. 1996. Relating extractable soil phosphorus to phosphorus losses in runoff. *Soil Sci. Soc. Am. J*. 60: 855-859.

Rinaldi, M., B. Mengoni, L. Luppi, S. E. Darby, and E. Mosselman, E., 2008. Numerical simulation of hydrodynamics and bank erosion in a river bend. *Water Resour. Res.* 44, (W09428) (doi:10.1029/2008WR007008).

Runkel, R. L., C. G. Crawford and T. A. Cohn. 2004. Load Estimator (LOADEST): a FORTRAN program for estimating constituent loads in streams and rivers. Techniques and Methods Book, Ch. A5. US Geological Survey, Reston, VA.

Sekely, A. C., D. J. Mulla and D. W. Bauer. 2002. Streambank slumping and its contribution to the Phosphorus and suspended sediment loads of the Blue Earth River, Minnesota. *J. Soil and Water Conserv.* 57(5): 243-250.

Simon, A., A. Curini, S. A. Darby and E. J. Langendoen. 2000. Bank and near-bank processes in an incised stream. *Geomorphology* 35: 193-217.

Simon, A., R. E. Thomas, and L. Klimetz. 2010. Comparison and experiences with field techniques to measure critical shear stress and erodibility of cohesive deposits. *2nd Joint Federal Interagency Conference*, Las Vegas, NV, June 27 – July 1, 2010.

Thorne, C. R. and N. K. Tovey. 1981. Stability of composite river banks. *Earth Surf. Proc. Land.* 6: 469-484.

Zaimes, G. N., R. C. Schultz and T. M. Isenhart. 2008. Streambank soil and phosphorus losses under different riparian land-uses in Iowa*. J. Am. Water Res. Assoc.* 44(4): 935-947.